



CMS-HIN-15-015

 CERN-EP/2016-242
 2017/04/13

Charged-particle nuclear modification factors in PbPb and pPb collisions at $\sqrt{s_{\text{NN}}} = 5.02 \text{ TeV}$

The CMS Collaboration^{*}

Abstract

The spectra of charged particles produced within the pseudorapidity window $|\eta| < 1$ at $\sqrt{s_{\text{NN}}} = 5.02 \text{ TeV}$ are measured using $404 \mu\text{b}^{-1}$ of PbPb and 27.4 pb^{-1} of pp data collected by the CMS detector at the LHC in 2015. The spectra are presented over the transverse momentum ranges spanning $0.5 < p_{\text{T}} < 400 \text{ GeV}$ in pp and $0.7 < p_{\text{T}} < 400 \text{ GeV}$ in PbPb collisions. The corresponding nuclear modification factor, R_{AA} , is measured in bins of collision centrality. The R_{AA} in the 5% most central collisions shows a maximal suppression by a factor of 7–8 in the p_{T} region of 6–9 GeV. This dip is followed by an increase, which continues up to the highest p_{T} measured, and approaches unity in the vicinity of $p_{\text{T}} = 200 \text{ GeV}$. The R_{AA} is compared to theoretical predictions and earlier experimental results at lower collision energies. The newly measured pp spectrum is combined with the pPb spectrum previously published by the CMS Collaboration to construct the pPb nuclear modification factor, R_{pA} , up to 120 GeV. For $p_{\text{T}} > 20 \text{ GeV}$, R_{pA} exhibits weak momentum dependence and shows a moderate enhancement above unity.

Published in the Journal of High Energy Physics as doi:10.1007/JHEP04(2017)039.

1 Introduction

The charged-particle transverse momentum (p_T) spectrum is an important tool for studying parton energy loss in the dense QCD medium, known as the quark gluon plasma (QGP), that is produced in high energy nucleus-nucleus (AA) collisions [1, 2]. In such collisions, high- p_T particles, which originate from parton fragmentation, are sensitive to the amount of energy loss that the partons experience traversing the medium. By comparing high- p_T particle yields in AA collisions to predictions of theoretical models, insight into the fundamental properties of the QGP can be gained. Over the years, a number of results have been made available by experiments at SPS [3, 4], at RHIC [5–8], and at the CERN LHC [9–11]. The modification of high- p_T particle production is typically quantified using the ratio of the charged-particle p_T spectrum in AA collisions to that of pp collisions, scaled by the average number of binary nucleon-nucleon collisions, $\langle N_{\text{coll}} \rangle$. This quantity is known as the nuclear modification factor, R_{AA} , and can also be formulated as function of p_T as

$$R_{\text{AA}}(p_T) = \frac{dN^{\text{AA}}/dp_T}{\langle N_{\text{coll}} \rangle dN^{\text{PP}}/dp_T} = \frac{dN^{\text{AA}}/dp_T}{T_{\text{AA}} d\sigma^{\text{PP}}/dp_T}, \quad (1)$$

where N^{AA} and N^{PP} are the charged-particle yields in AA collisions and pp collisions, and σ^{PP} is the charged-particle cross section in pp collisions. The ratio of $\langle N_{\text{coll}} \rangle$ with the total inelastic pp cross section, defined as $T_{\text{AA}} = \langle N_{\text{coll}} \rangle / \sigma_{\text{inel}}^{\text{PP}}$, is known as the nuclear overlap function and can be calculated from a Glauber model of the nuclear collision geometry [12]. In this work we adopt natural units, such that $c = 1$.

The factor of 5 suppression observed in the R_{AA} of charged hadrons and neutral pions at RHIC [5–8] was an indication of strong medium effects on particle production in the final state. However, the RHIC measurements were limited to a p_T range below 25 GeV and a collision energy per nucleon pair, $\sqrt{s_{\text{NN}}}$, less than or equal to 200 GeV. The QGP is expected to have a size, lifetime, and temperature that are affected by the collision energy. During the first two PbPb runs, the LHC collaborations measured the charged-particle R_{AA} at $\sqrt{s_{\text{NN}}} = 2.76$ TeV, up to p_T around 50 GeV (ALICE [9]), 100 GeV (CMS [11]), and 150 GeV (ATLAS [10]). A suppression by a factor of about 7 was observed in the 5–10 GeV p_T region [9–11]. At higher p_T , the suppression was not as strong, approaching roughly a factor of 2 for particles with p_T in the range of 40–100 GeV. At the end of 2015, in the first heavy ion data-taking period of the Run-2 at the LHC, PbPb collisions at $\sqrt{s_{\text{NN}}} = 5.02$ TeV took place, allowing the study of the suppression of charged particles at a new collision energy frontier. Proton-proton data at the same collision energy were also taken, making direct comparison between particle production in pp and PbPb collisions possible.

To gain access to the properties of the QGP, it is necessary to separate the effects directly related to the hot partonic QCD system from those referred to as cold nuclear matter effects. Measurements in proton-nucleus collisions can be used for this purpose. The CMS Collaboration has previously published results for the nuclear modification factor R_{pA}^* using measured charged-particle spectra in pPb collisions at $\sqrt{s_{\text{NN}}} = 5.02$ TeV and a pp reference spectrum constructed by interpolation from previous measurements at higher and lower center-of-mass energies [13]. The asterisk in the notation refers to this usage of an interpolated reference spectrum. Similarly interpolation-based results are also available from the ATLAS [14] and the ALICE [15] experiments. With the pp data taken in 2015 at $\sqrt{s} = 5.02$ TeV, the measurement of the nuclear modification factor, R_{pA} , using a measured pp reference spectrum, becomes possible.

In this paper, the spectra of charged particles in the pseudorapidity window $|\eta| < 1$ in pp and PbPb collisions at $\sqrt{s_{\text{NN}}} = 5.02$ TeV, as well as the nuclear modification factors, R_{AA} and R_{pA} ,

are presented. Throughout this paper, for each collision system, the pseudorapidity is computed in the center-of-mass frame of the colliding nucleons. The measured R_{AA} is compared to model calculations, as well as to previous experimental results at lower collision energies.

2 The CMS detector and data selection

The central feature of the CMS apparatus is a superconducting solenoid of 6 m internal diameter, providing an axial magnetic field of 3.8 T. Within the solenoid volume are a silicon pixel and strip tracker covering the range of $|\eta| < 2.5$ [16], a lead tungstate crystal electromagnetic calorimeter, and a brass and scintillator hadron calorimeter, each composed of a barrel and two endcap sections. Hadron forward calorimeters (HF), consisting of steel with embedded quartz fibers, extend the calorimeter coverage up to $|\eta| < 5.2$. Muons are measured in gas-ionization detectors embedded in the steel flux-return yoke outside the solenoid. A more detailed description of the CMS detector, together with a definition of the coordinate system used and the relevant kinematic variables, can be found in Ref. [16].

The measurement of R_{AA} is performed using the 2015 pp and PbPb data taken at $\sqrt{s_{\text{NN}}} = 5.02 \text{ TeV}$. The pp sample corresponds to an integrated luminosity of 27.4 pb^{-1} , while the PbPb sample corresponds to an integrated luminosity of $404 \mu\text{b}^{-1}$. For pp collisions the average pileup (the mean of the Poisson distribution of the number of collisions per bunch crossing) was approximately 0.9. For the measurement of R_{pA} , 35 nb^{-1} of $\sqrt{s_{\text{NN}}} = 5.02 \text{ TeV}$ pPb data are used.

The collision centrality in PbPb events, i.e. the degree of overlap of the two colliding nuclei, is determined from the total transverse energy, E_{T} , deposition in both HF calorimeters. Collision-centrality bins are given in percentage ranges of the total hadronic cross section, 0–5% corresponding to the 5% of collisions with the largest overlap of the two nuclei. The collision centrality can be related to properties of the PbPb collisions, such as the total number of binary nucleon-nucleon collisions, N_{coll} . The calculation of these properties is based on a Glauber model of the incoming nuclei and their constituent nucleons [12, 17], as well as studies of bin-to-bin smearing, which is evaluated by examining the effects of finite resolution on fully simulated and reconstructed events [18]. The calculated average N_{coll} and T_{AA} values corresponding to the centrality ranges used, along with their systematic uncertainties, are listed in Table 1. The $\sigma_{\text{inel}}^{\text{pp}}$ utilized in the Glauber calculation is $70 \pm 5 \text{ mb}$ [19]. The nuclear radius and skin depth are $6.62 \pm 0.06 \text{ fm}$ and $0.546 \pm 0.010 \text{ fm}$, respectively, and a minimal distance between nucleons of $0.04 \pm 0.04 \text{ fm}$ is imposed [20]. In this paper, only T_{AA} is used in the calculation of R_{AA} , as given by the last formula in Eq. (1).

The CMS online event selection employs a hardware-based level-1 trigger (L1) and a software-based high-level trigger (HLT). Minimum-bias pp and PbPb collisions were selected using an HF-based L1 trigger requiring signals above threshold in either one (pp) or both (PbPb) sides of HF calorimeters. These data were utilized to access the low- p_{T} kinematic region of charged particles. In order to extend the p_{T} reach of the results reported in this paper, events selected by jet triggers were used. High- p_{T} track triggers were also employed, but only as a cross-check of the result obtained with jet triggers.

At the L1 stage, the jet-triggered events in pp and PbPb collisions were selected by requiring the presence of L1-reconstructed jets above various E_{T} thresholds, listed in Table 2. While the lower-threshold triggers had to be prescaled because of the high instantaneous luminosity of the LHC, the highest threshold trigger was always unprescaled. In PbPb collisions, the L1 jet trigger algorithms performed an online event-by-event underlying-event subtraction, estimat-

Table 1: The values of $\langle N_{\text{coll}} \rangle$ and T_{AA} and their uncertainties in $\sqrt{s_{\text{NN}}} = 5.02 \text{ TeV}$ PbPb collisions for the centrality ranges used in this paper.

Centrality	$\langle N_{\text{coll}} \rangle$	$T_{\text{AA}} [\text{mb}^{-1}]$
0–5%	1820^{+130}_{-140}	$26.0^{+0.5}_{-0.8}$
5–10%	1430^{+100}_{-110}	$20.5^{+0.4}_{-0.6}$
10–30%	805^{+55}_{-58}	$11.5^{+0.3}_{-0.4}$
30–50%	267^{+20}_{-20}	$3.82^{+0.21}_{-0.21}$
50–70%	$65.4^{+7.0}_{-6.6}$	$0.934^{+0.096}_{-0.089}$
70–90%	$10.7^{+1.7}_{-1.5}$	$0.152^{+0.024}_{-0.021}$
0–10%	1630^{+120}_{-120}	$23.2^{+0.4}_{-0.7}$
0–100%	393^{+27}_{-28}	$5.61^{+0.16}_{-0.19}$

Table 2: Summary of the E_{T} and p_{T} thresholds of the various L1 and HLT triggers used in the analysis for the two colliding systems. Please refer to the text about the exact meaning of the thresholds. Only the highest-threshold triggers collected data unprescaled. The MB symbol refers to seeding by a minimum-bias trigger.

Collision system/trigger	L1 thresholds [GeV]	HLT thresholds [GeV]
pp		
Jet triggers	28, 40, 48	40, 60, 80
Track triggers	MB, 28, 40, 48	12, 24, 34, 45, 53
PbPb		
Jet triggers	28, 44, 56	40, 60, 80, 100
Track triggers	MB, 16, 24	12, 18, 24, 34

ing the energy of the underlying event by averaging the deposited calorimeter E_{T} in rings of azimuthal angle (ϕ , in radians) as a function of η , for each event separately. Events triggered by high- p_{T} tracks in pp collisions were selected by the same L1 jet triggers as described above. In PbPb collisions, a special algorithm based on the E_{T} of the highest- E_{T} underlying-event subtracted calorimeter trigger region ($\Delta\eta$, $\Delta\phi = 0.348$) in the central ($|\eta| < 1.044$) detector area was employed. The presence of a high- p_{T} track is better correlated with the presence of a high- E_{T} trigger region than with the presence of a multiregion-wide L1 jet. Therefore, seeding the high- p_{T} track triggers with the former algorithm leads to a lower overall L1 trigger rate. This was an important consideration in PbPb collisions, while it had much less importance in pp ones. Both the jet and the track triggers had variants selecting only PbPb collision events of specific centralities. This was made possible by an L1 algorithm, which estimated the collision centrality based on the sum of the E_{T} deposited in the HF calorimeter regions. The measurement of PbPb spectra reported in this paper makes use of such triggers to increase the number of events in peripheral centrality bins.

At the HLT, online versions of the pp and PbPb offline calorimeter jet and track reconstruction algorithms were run. In pp collisions, events selected by high-level jet triggers contain calorimeter clusters which are above various p_{T} values (Table 2) in the $|\eta| < 5.1$ region. Such clusters were produced with the anti- k_{T} algorithm [21, 22] of distance parameter $R=0.4$, and were corrected to establish a relative uniform calorimeter response in η and a calibrated absolute response in p_{T} . In this configuration, the 80 GeV threshold trigger was unprescaled. In PbPb collisions, the $R=0.4$ anti- k_{T} calorimeter jets were clustered and corrected after the energy due to the heavy-ion underlying event was subtracted in an η -dependent way [23]. Triggers with thresholds on the jet energy from 40 to 100 GeV were employed. The independent high-

p_T track triggers looked for a track in the $|\eta| < 2.4$ (pp) and $|\eta| < 1.05$ (PbPb) regions above different p_T thresholds, listed in Table 2.

Events selected for offline analysis are required to pass a set of selection criteria designed to reject events from background processes (beam-gas collisions and beam scraping events). Events are required to have at least one reconstructed primary interaction vertex with at least two associated tracks. In pp collisions, the events are also required to have at least 25% of the tracks passing a tight track-quality selection requirement [24]. In PbPb collisions, the shapes of the clusters in the pixel detector are required to be compatible with those expected from particles produced by a PbPb collision. The PbPb collision event is also required to have at least three towers in each of the HF detectors with energy deposits of more than 3 GeV per tower.

3 Track reconstruction and corrections

The distributions reported in this paper are for primary charged particles. Primary charged particles are required to have a mean proper lifetime greater than 1 cm. The daughters of secondary decays are considered primary only if the mother particle had a mean proper lifetime less than 1 cm. Additionally, charged particles resulting from interactions with detector material are not considered primary particles.

The track reconstruction used in pp collisions for this study is described in Ref. [24]. In PbPb collisions, minor modifications are made to the pp algorithm in order to accommodate the much larger track multiplicities. Only tracks in the range $|\eta| < 1$ are used. Tracks are required to have a relative p_T uncertainty of less than 10% in PbPb collisions and 30% in pp collisions. In PbPb collisions, tracks must also have at least 11 hits and satisfy a stringent fit quality requirement, specifically that the χ^2 , divided by both the number of degrees of freedom and the number of tracker layers hit, be less than 0.15. To decrease the likelihood of counting nonprimary charged particles originating from secondary decay products, a selection requirement of less than 3 standard deviations is applied on the significance of the distance of closest approach to at least one primary vertex in the event, for both collision systems. Finally, a selection based on the relationship of a track to calorimeter energy deposits along its trajectory is applied in order to curtail the contribution of misreconstructed tracks with very high p_T . Tracks with $p_T > 20$ GeV are required to have an associated energy deposit [25] of at least half their momentum in the CMS calorimeters. This requirement was determined by comparing the distributions of the associated deposits for genuine and misreconstructed tracks in simulated events to tracks reconstructed in real data. The efficiency of the calorimeter-matching requirement is 98% (95%) in PbPb (pp) data for tracks selected for analysis by the previously mentioned other track selection criteria.

To correct for inefficiencies associated with the track reconstruction algorithms, simulated Monte Carlo (MC) samples are used. For pp collision data, these are generated with PYTHIA 8.209 [26] tune CUETP8M1 [27] minimum-bias, as well as QCD dijet samples binned in the transverse momentum of the hard scattering, \hat{p}_T . For PbPb collision data, HYDJET 1.9 [28] minimum-bias events and HYDJET-embedded PYTHIA QCD dijet events are used. In the embedding procedure, a high- \hat{p}_T PYTHIA event is combined with a minimum-bias HYDJET event with the same vertex location. The combined event is then used as input to the full simulation of the CMS detector response.

In general the tracking efficiency, defined as the fraction of primary charged particles successfully reconstructed, is non-unitary due to algorithmic inefficiencies and detector acceptance effects. Furthermore, misreconstruction, where a track not corresponding to any charged particle

is errantly reconstructed, can inject extra tracks into the analysis. Finally, tracks corresponding to products of secondary interactions or decays, which still pass all track selection criteria and are therefore selected for analysis, must also be taken into account. Corrections for these effects are applied on a track-by-track basis, and take into consideration the properties of each track: p_T , η , ϕ , and radial distance of the track from the closest jet axis. The functional dependence of the corrections is assumed to factorize into the product of four single-variable functions in separate classes of track kinematics properties. This factorization is only approximate because of correlations between the variables. These correlations are accounted for in a systematic uncertainty. The tracking efficiency in pp is between 80 and 90% for most of the p_T range studied, except for $p_T > 150$ GeV, where it decreases to 70%. The pp track misreconstruction rate and secondary rate are found to be less than 3% and 1%, respectively, in each p_T bin examined. Owing to the dependence of the tracking efficiency on detector occupancy, the event centrality is also taken into account in the correction procedure for PbPb collisions. Additionally, to account for the slightly different χ^2/dof in data and simulated events, a track-by-track reweighting is applied to the simulation during this calculation. The efficiency of the PbPb track reconstruction algorithm and track selection criteria for minimum-bias events is approximately 40% at 0.7 GeV. It then increases rapidly to around 65% at 1 GeV, where it reaches a plateau. It starts to decrease from p_T values of around 100 GeV until it reaches about 50% at 400 GeV. This efficiency is also centrality dependent; the p_T -inclusive value is approximately 60% for central events and 75% for peripheral events. In general, the PbPb misreconstruction and secondary rates are very small because of the strict selection criteria applied to the tracks. The misreconstruction rate does increase at low track p_T and also slightly at very high p_T , to around 1.5%. Below 1 GeV it increases to 10% for the most central events. These numbers are in line with the expected tracking performance based on previous studies of similar tracking algorithms in pp collisions at $\sqrt{s} = 7$ TeV [24] and PbPb collisions at $\sqrt{s_{\text{NN}}} = 2.76$ TeV [29].

Particles of different species have different track reconstruction and selection efficiencies at the same p_T . As different MC event generators model the relative fractions of the particle species differently, the computed tracking efficiencies for inclusive primary charged particles depend on which MC generator is used to evaluate the correction. Notably, the reconstruction efficiency for primary charged strange baryons is very low, as they decay before leaving a sufficient number of tracker hits for direct reconstruction. In this measurement, the species-dependent track reconstruction efficiencies are first calculated and then weighted with the corresponding particle fractions produced by PYTHIA 8, tune CUETP8M1 and EPOS [30], tune LHC [31]. PYTHIA is expected to underpredict the fraction of strange baryons present in PbPb collisions, while EPOS overpredicts strange baryon production in central collisions at lower collision center-of-mass energies [32]. Therefore we choose a working point between these two models by averaging the two sets of correction factors.

The p_T resolution of selected tracks in both pp and PbPb collisions remains below 2% up to 100 GeV. For higher p_T it starts to increase, reaching about 6% at 400 GeV. The resulting change in the measured charged-particle yields introduced by the track resolution is found to be less than 1%. A correction is not made for this distortion, but rather the distortion is accounted for in the systematic uncertainty.

The distortion of the shape of the pp p_T distribution due to the event selection requirements is calculated by evaluating the efficiency of the selection in “zero bias” data. Zero bias data were selected solely based on whether there were filled bunches in both beams crossing each other in the CMS interaction region. Therefore, the zero bias data set provides an unbiased sample to study the efficiency of the minimum-bias trigger and of the offline event selection. As a result of this study, a correction is applied for a small (less than 1%) distortion of the very low-

p_T spectrum due to valid events failing to pass the event selection. For the PbPb sample, the event selection is fully efficient from 0 to 90% event centrality classes. For quantities inclusive in centrality, the event selection efficiency of $99 \pm 2\%$ is corrected for. (Selection efficiencies higher than 100% are possible, reflecting the presence of ultra-peripheral collisions in the selected event sample.)

4 Combination of data from different triggers

To obtain the inclusive charged-particle spectra up to a few hundred GeV of transverse momenta, data recorded by the minimum-bias and jet triggers are combined. The procedure is outlined in Refs. [11, 13].

The event-weighting factors corresponding to the various triggers are computed by counting the number of events that contain a leading jet (defined as the jet with the highest p_T in the event) in the range of $|\eta| < 2$ with p_T values in regions not affected by trigger thresholds. In these regions, the trigger efficiency of the higher-threshold trigger is constant relative to that of the lower-threshold trigger. The ratio of the number of such events in the two triggered sets of data is used as a weighting factor. For example, the region above which the jet trigger with a p_T threshold of 40 GeV has constant efficiency is determined by comparing the p_T distribution of the leading jets to that of the minimum-bias data. Similarly, the constant efficiency region of the 60 GeV jet trigger is determined by comparison to the 40 GeV jet trigger, etc.

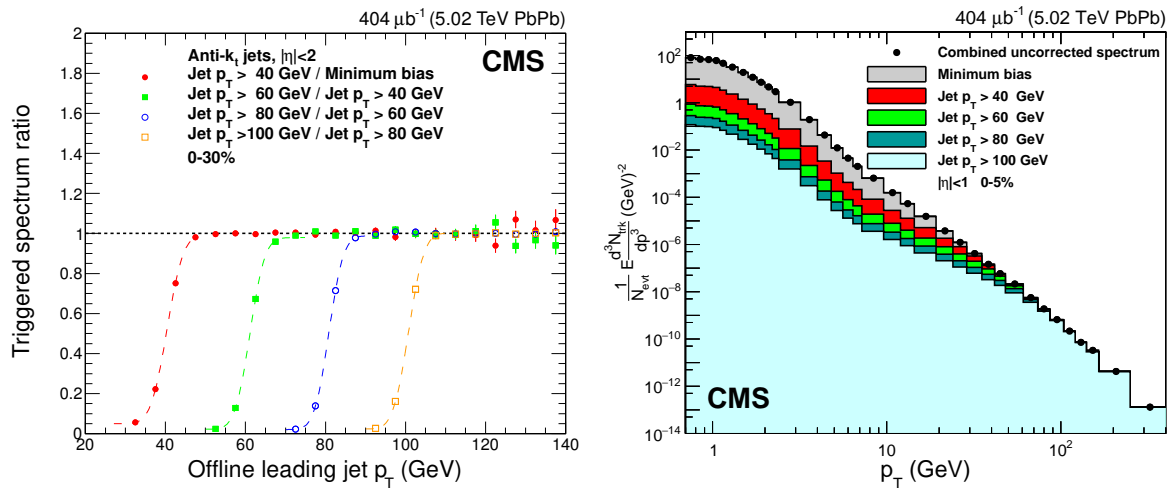


Figure 1: Left: ratio of the leading jet p_T distributions in PbPb collisions in the 0–30% centrality range from various triggers, after the data have been normalized to one another. Lines have been added to guide the eye. Right: contributions from the various jet triggers (colored histograms) to the combined, but otherwise uncorrected, track spectrum (black markers) in the 0–5% centrality range in PbPb collisions. The statistical uncertainties are smaller than the size of the data markers.

To determine the inclusive particle spectrum, events are first uniquely classified into leading jet p_T classes. The pp spectra are constructed by taking events from the minimum-bias, 40 GeV jet, 60 GeV jet, 80 GeV jet, and 100 GeV jet triggers, for each respective class. The particle spectra are evaluated in each class separately, and then combined using the normalization factors described in the previous paragraph. The procedure outlined above is verified by constructing a charged-particle spectrum from an alternative combination of event samples triggered by high- p_T track triggers. The final spectra are found to be consistent with each other. In PbPb

collisions, the overall normalization of the combined spectrum is performed using the number of minimum-bias events in the appropriate centrality range. In pp collisions, the normalization is set by the integrated luminosity.

The ratio of the normalized distribution of the leading jet p_T from minimum-bias and from various jet-triggered data in PbPb collisions in the 0–30% centrality range can be seen in the left panel of Fig. 1. The constant-efficiency regions are selected to be above p_T of 60, 80, 100, and 120 GeV for the triggers having a threshold of 40, 60, 80, and 100 GeV, respectively. The contribution from each of the data sets selected by the different jet trigger thresholds to the combined, but otherwise uncorrected, track spectrum in the 0–5% centrality range can be seen in the right panel of Fig. 1. The combined spectrum includes contributions from each jet trigger threshold data set at each charged-particle p_T bin, although the relative contributions of the different data sets naturally vary strongly as a function of p_T .

The scheme outlined above is slightly modified for the combination of the spectra using events from the 0–30% centrality range. In that range, due to the large minimum-bias data set and the absence of the peripheral-specific jet triggers (see Section 2), the minimum-bias data provide higher statistical power than the data triggered with the 40 GeV jet trigger. Thus, the data from this jet trigger path are not used, and the minimum-bias sample is combined with the higher-threshold jet-triggered sample. The 40 GeV jet trigger is shown in Fig. 1 for illustration.

5 Systematic uncertainties

The systematic uncertainties influencing the measurement of the spectra of charged particles in pp and PbPb collisions as well as the R_{AA} are presented in Table 3. The ranges quoted cover both the p_T and the centrality dependence of the uncertainties. In the following, each source of systematic uncertainty is discussed separately, including a discussion on the cancellation of the spectra uncertainties in R_{AA} .

- Particle species composition. As described in Section 3, the tracking corrections used in the analysis correspond to a particle species composition that lies halfway between that from PYTHIA 8, tune CUETP8M1 and EPOS, tune LHC. We assign the difference between these corrections and the corrections given by the PYTHIA 8 or the EPOS particle compositions as a systematic uncertainty in the pp and PbPb spectra. The systematic uncertainty has a strong p_T dependence, directly related to how much the two models differ at a given p_T . Below a p_T of around 1.5 GeV, the uncertainty is 1% both in pp and PbPb data. For higher p_T , the uncertainty increases rapidly with p_T , reaching a value of about 8% (pp) and 13.5% (PbPb in the 0–5% centrality range) at 3 GeV, followed by a steady decrease to 1% at and above 10 GeV. The uncertainties are evaluated in bins of centrality, resulting in higher uncertainties for more central events. For R_{AA} , the conservative assumption of no cancellation of this uncertainty is made, resulting in uncertainty values between 1.5 and 15.5%.
- MC/data tracking efficiency difference. The difference in the track reconstruction efficiency in pp data and pp simulation was studied by comparing the relative fraction of reconstructed D^* mesons in the $D^* \rightarrow D\pi \rightarrow K\pi\pi$ and $D^* \rightarrow D\pi \rightarrow K\pi\pi\pi\pi$ decay channels in simulated and data events, following Ref. [33]. Additional comparisons were made between track quality variables before track selections in both pp and PbPb data and simulation. Based on these two studies, p_T -independent uncertainties of 4% (pp) and 5% (PbPb) are assigned.

To study the potential cancellation of the pp and PbPb uncertainties in R_{AA} , an ex-

amination of the relative difference between pp and PbPb of MC/data tracking efficiency discrepancies is performed. First, the ratio of the uncorrected track spectra in data in the 30–100% centrality bin is computed using the pp and the PbPb reconstruction algorithms. The same ratio is also evaluated using MC events as inputs. Finally, the ratio of the previously-computed MC and data ratios is constructed. Assuming that the misreconstruction rate in data and MC is the same, this double ratio is proportional to the relative MC/data tracking efficiency difference between pp and PbPb. Small differences between data and MC, which break the assumption on the misreconstruction rate, are accounted for with the “fraction of misreconstructed tracks” systematic uncertainty discussed later in this section. Based on this study, an uncertainty ranging from 2% (70–90% centrality bin) to 6.5% (0–30% centrality bins) is assigned to the R_{AA} measurement.

Table 3: Systematic uncertainties associated with the measurement of the charged-particle spectra and R_{AA} using $\sqrt{s_{NN}} = 5.02$ TeV pp and PbPb collision data. The ranges quoted cover both the p_T and the centrality dependence of the uncertainties. The combined uncertainty in R_{AA} does not include the integrated luminosity and the T_{AA} uncertainties.

Sources	Uncertainty [%]		
	pp	PbPb	R_{AA}
Particle species composition	1–8	1.0–13.5	1.5–15.5
MC/data tracking efficiency difference	4	4–5	2.0–6.5
Tracking correction procedure	1	1–4	1.5–4.0
PbPb track selection	—	4	4
Pileup	3	<1	3
Fraction of misreconstructed tracks	<3	<1.5	<3
Trigger combination	<1	1	1
Momentum resolution	1	1	1
Event selection correction	<1	—	<1
Combined uncertainty	7–10	7–15	7.0–17.5
Glauber model uncertainty (T_{AA})	—	—	1.8–16.1
Integrated luminosity	2.3	—	2.3

- Tracking correction procedure. The accuracy of the tracking correction procedure is tested in simulated events by comparing the fully corrected track spectrum to the spectrum of simulated particles. In such comparisons, differences smaller than 1% (pp) and 3% (PbPb) are observed. The main source of the differences is the fact that the tracking efficiency only approximately factorizes into single-variable functions of track p_T , track η and ϕ , event centrality, and radial distance of the tracks from jets in the bins of track p_T and event centrality used for the calculation of the tracking correction factors. Such differences in the tracking corrections are one of the two sources of systematic uncertainty in the derivation of tracking correction factors considered in this analysis. The second source of systematic uncertainty is related to only having a limited number of simulated events to determine the correction factors. While this uncertainty for pp collisions is negligible, for PbPb collisions it can reach 3% and is accounted for in a p_T and centrality-dependent way. No cancellation of the tracking correction uncertainties in pp and PbPb collisions is assumed in the computation of R_{AA} .
- PbPb track selection. The track selection criteria are stricter in PbPb than in pp collisions. Selecting on more track quality variables naturally introduces a larger dependence on the underlying MC/data (dis)agreement for the track quality vari-

ables in question. To study the effect of such disagreements, the reconstruction of charged-particle spectra was repeated using looser track selection criteria. Based on the differences observed in the fully corrected spectra, an uncertainty of 4% is assigned for the PbPb spectra, as well as in R_{AA} .

- Pileup. In this analysis, tracks compatible with any of the primary vertices are selected. To assess the possible effect of pileup on the particle spectrum, the spectrum was recomputed using only single-vertex collision events. Based on the differences observed in the shape of the spectra, a systematic uncertainty of 3% is evaluated. For PbPb collisions, the much smaller pileup is found to have a negligible effect on the reported charged-particle spectra. Consequently, the 3% uncertainty in the pp spectrum is propagated to R_{AA} .
- Fraction of misreconstructed tracks. The fraction of misreconstructed tracks is computed from simulated events. To account for possible differences in the misreconstruction fraction between simulated and data events, the total amount of the corrections, less than 3% in pp and less than 1.5% in PbPb collisions, is assigned as a systematic uncertainty in the charged-particle spectra in a p_T -dependent fashion. These uncertainties are conservatively assumed to not cancel for the calculation of the uncertainty in R_{AA} .
- Trigger combination. The method of combining the different triggers used in this analysis relies on the calculation of overlaps in the leading jet spectra between the different triggers. The calculated trigger weights are subject to statistical fluctuations due to a statistically limited data sample. To assess the corresponding uncertainty in R_{AA} , the uncertainties on the trigger weights associated to each trigger path are weighted according to the fraction of the particle spectrum that the trigger contributes in a given p_T bin. The overall uncertainty is found to range from negligible to 1%. The uncertainty is highest for peripheral events and increases with p_T .
- Momentum resolution. The variation of the yield of charged particles in any given p_T bin due to the finite resolution of the track reconstruction is evaluated using simulated events. The yields are found to only change by around 1% both in pp and PbPb collisions. For R_{AA} , the same 1% systematic uncertainty is conservatively assigned.
- Event selection correction. The bias resulting from the event selection conditions on the shape of the pp spectrum and R_{AA} distributions is corrected by a procedure, which directly evaluates the event selection efficiency based on zero-bias data alone (see Section 3). To estimate the corresponding systematic uncertainty, the event selection correction is also evaluated using simulated events. The charged-particle p_T distribution in pp and the R_{AA} distribution, reconstructed with the MC-based alternative event selection correction, are found to differ by less than 1% from the main result. For centrality-inclusive PbPb quantities, an uncertainty due to event selection is combined with the T_{AA} uncertainty.
- Glauber model uncertainty. The systematic uncertainty in the Glauber model normalization factor (T_{AA}) ranges from 1.8% (in the 0–5% centrality bin) to 16.1% (in the 70–90% centrality bin). The uncertainties in the T_{AA} values are derived from propagating the uncertainties in the event selection efficiency, and in the nuclear radius, skin depth, and minimum distance between nucleons in the Pb nucleus [20] parameters of the Glauber model.
- Integrated luminosity. The uncertainty in the integrated luminosity for pp collisions is 2.3%. For the PbPb analysis, no luminosity information is used as per-event yields are measured.

6 Results

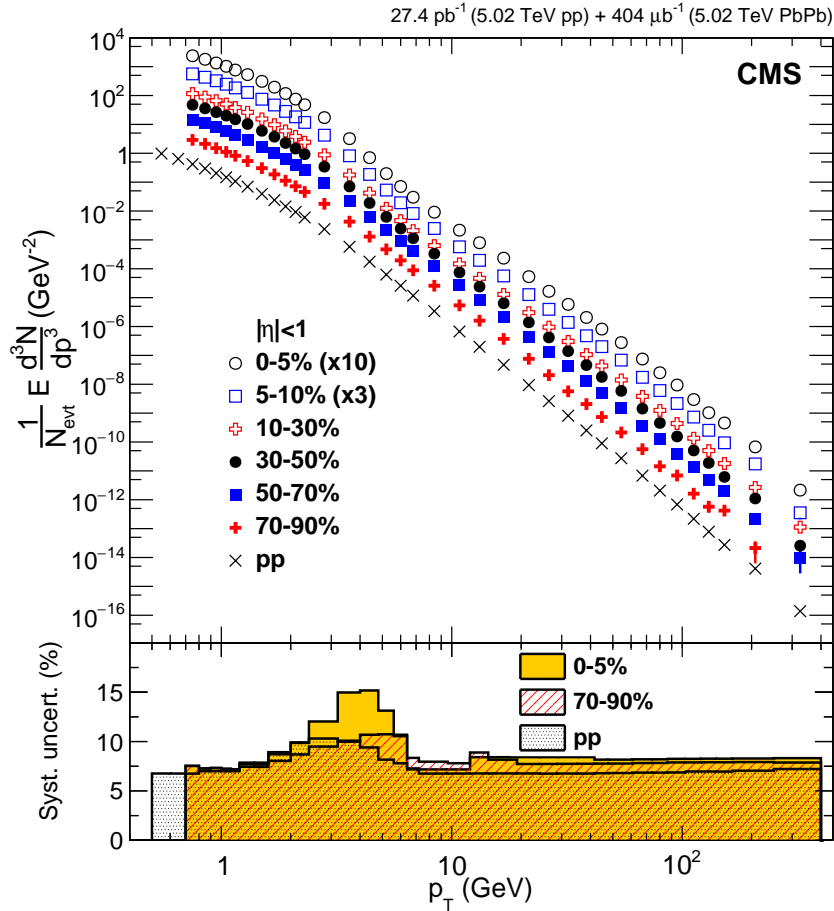


Figure 2: (Top panel) Charged-particle per-event yields measured in various PbPb centrality classes, as well as in pp data. A factor of 70 mb is used to scale the pp spectrum from a differential cross section to a per-event yield for direct comparison. The statistical uncertainties are smaller than the size of the markers for most points. (Bottom panel) Systematic uncertainties as a function of p_T for representative data sets. The pp uncertainty contains a 2.3% fully correlated uncertainty in the pp integrated luminosity.

The measured charged-particle spectra are shown in Fig. 2 for both pp and PbPb collisions at $\sqrt{s_{\text{NN}}} = 5.02$ TeV. The PbPb results are shown in the 0–5%, 5–10%, 10–30%, 30–50%, 50–70%, and 70–90% centrality ranges, and are given as per-event differential yields. The two most central bins have been scaled by constant factors of three and ten for visual clarity. The pp spectrum, for the purposes of measuring the R_{AA} , is measured as a differential cross section. In order to convert this quantity to a per-event yield for comparison on the same figure, a scaling factor of 70 mb, corresponding approximately to the total inelastic pp cross section, is applied. No correction is applied for the finite size of the p_T bins; the points represent the average yield across the bin. The spectrum in pp collisions resembles a power law beyond a p_T of around 5 GeV. In comparison, the spectra in central PbPb collisions are visibly modified, leading to p_T -dependent structures in R_{AA} . Representative systematic uncertainties are shown in the lower panel for central and peripheral PbPb data, as well as for the pp data. The pp uncertainty shown includes a 2.3% correlated uncertainty coming from the use of the pp integrated luminosity in the determination of the spectrum normalization.

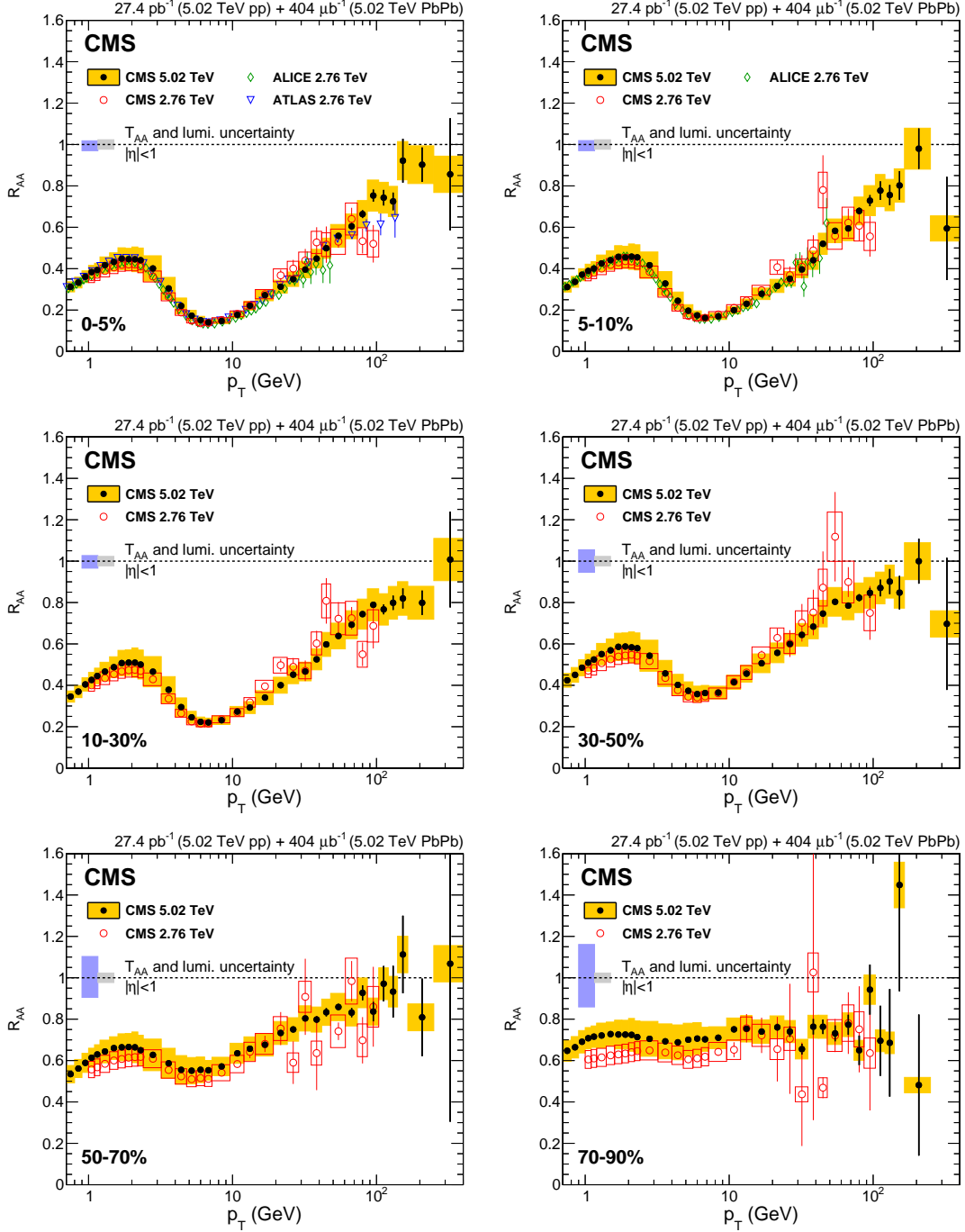


Figure 3: Charged-particle R_{AA} measured in six different centrality ranges at $\sqrt{s_{NN}} = 5.02$ TeV compared to results at $\sqrt{s_{NN}} = 2.76$ TeV from CMS [11] (all centrality bins), ALICE [9] (in the 0–5% and 5–10% centrality ranges), and ATLAS [10] (in the 0–5% centrality range). The yellow boxes represent the systematic uncertainty of the 5.02 TeV CMS points.

The measured nuclear modification factors for primary charged particles in PbPb collisions are shown in Fig. 3. The error bars represent statistical uncertainties. The blue and gray boxes around unity show the T_{AA} and pp luminosity uncertainties, respectively, while the yellow band represents the other systematic uncertainties as discussed in Section 5. The R_{AA} distributions show a characteristic suppression pattern over most of the p_T range measured, having local maxima at about a p_T of 2 GeV and local minima at around 7 GeV. These features are

much stronger for central collisions than for peripheral ones, and are presumably the result of the competition between nuclear parton distribution function effects [34], radial flow [35], parton energy loss, and the Cronin effect [36, 37], which all depend upon centrality. The suppression seen for 0–5% collisions is about 7–8 for p_T of around 6–9 GeV. Above these p_T values, radial flow is insignificant and the shape of R_{AA} is expected to be dominated by parton energy loss. At larger p_T , R_{AA} appears to exhibit a continuous rise up to the highest p_T values measured, with R_{AA} values approaching unity. On the other hand, the R_{AA} for the 70–90% centrality class displays relatively little p_T dependence. It is approximately centered around 0.75, albeit with a large systematic uncertainty which is dominated by a 16.1% contribution from the T_{AA} uncertainty. In all centrality classes, the uncertainties show a characteristic increase in the 2–10 GeV p_T region driven by the uncertainty due to the particle composition, which is largest in that region (see Section 5).

The measured R_{AA} distributions at $\sqrt{s_{NN}} = 5.02$ TeV are also compared to the CMS measurements at $\sqrt{s_{NN}} = 2.76$ TeV [11] in Fig. 3. Additionally, for the 0–5% and 5–10% bins, results from one or both of the ALICE [9] and ATLAS [10] collaborations are shown. The error bars represent the statistical uncertainties, while the boxes indicate all systematic uncertainties, other than the luminosity and T_{AA} uncertainties, for both CMS measurements. The 2.76 TeV CMS measurement has a 6% pp luminosity uncertainty and a T_{AA} uncertainty, which is similar to that for 5.02 TeV [11]. The measured R_{AA} distributions at 2.76 and 5.02 TeV are quantitatively similar to each other. At p_T values below about 7 GeV, the 5.02 TeV data tend to be higher, however the difference is mostly covered by the systematic uncertainties of the respective measurements. It is worth noting that because of the different particle composition corrections applied in pp and PbPb at 5.02 TeV, the R_{AA} is shifted upward by 1 to 5% in the p_T region of 1–14 GeV compared to an R_{AA} , where no such correction is applied, such as the 2.76 TeV CMS result. Above about 10 GeV and for central collisions, the 5.02 TeV R_{AA} tends to be slightly smaller than the 2.76 TeV one. For peripheral collisions, we see the opposite trend.

Figure 4 shows a comparison of the measured R_{AA} distributions in the 0–10% and 30–50% centrality ranges to the predictions from models described in Refs. [38–43]. The SCET_G model [38] is based on the generalization of the DGLAP evolution equations to include final-state medium-induced parton showers combined with initial-state effects. This model gives a good description of the measured data over the full p_T range of the prediction, for p_T between 5 and 200 GeV. In the Hybrid model [39], the in-medium rate of energy loss is predicted using a strongly coupled theory. This parametrization is then used to retroactively modify the particle shower produced by PYTHIA 8.183. Hadronization is accomplished using the PYTHIA implementation of the Lund string model [44]. The model tends to predict less suppression than the other models considered here, but is consistent with the measured data. The model of Bianchi et al. [40] attempts to use the scale-dependence of the QGP parton distribution function to describe data at both RHIC and the LHC. The calculation allows the medium transport coefficient, \hat{q} , to vary with the energy scale of jets traversing the medium. Although the model agrees with the data well at high p_T , some discrepancy can be seen at the lower p_T range of the prediction. The CUJET 3.0 model [41] is constructed by generalizing the perturbative-QCD-based CUJET 2.0 model built upon the Gyulassy–Levai–Vitev opacity series formalism [45]. These generalizations include two complementary nonperturbative features of the QCD confinement cross-over phase transition: suppression of quark and gluon degrees of freedom, and the emergence of chromomagnetic monopoles. For central collisions, the model predicts a suppression for charged hadrons plus neutral pions that is larger than seen in the data for charged particles. In the 30–50% centrality bin, however, the model is compatible with most of the data points. The prediction by Andrés et al. [42] comes from using the ‘quenching weights’ formalism and fitting a

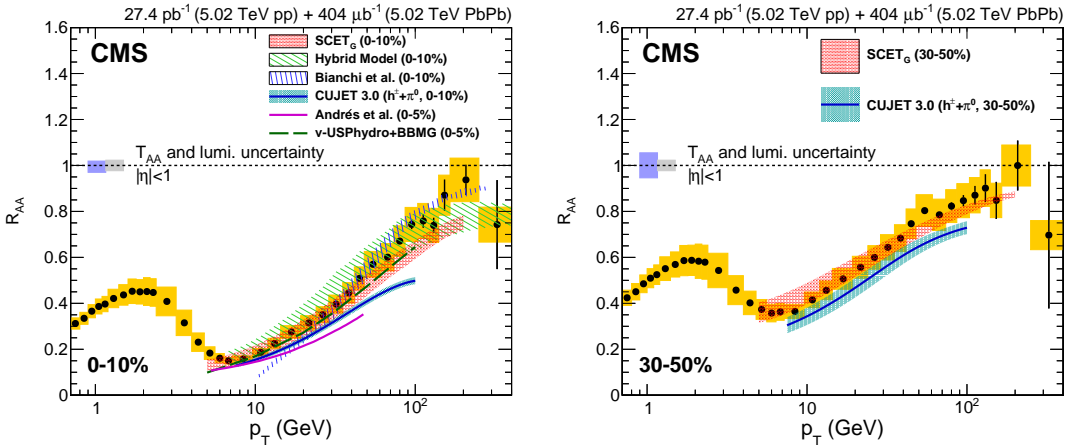


Figure 4: Charged-particle R_{AA} measured in the 0–10% (left) and 30–50% (right) centrality ranges at $\sqrt{s_{NN}} = 5.02$ TeV compared to predictions of models from Refs. [38–43]. The yellow band represents the systematic uncertainty of the 5.02 TeV CMS points.

K factor to the inclusive particle suppression at LHC energies to parametrize the departure of \hat{q} from an ideal estimate. The K factor used to determine the predicted suppression at 5.02 TeV is assumed to be the same as the one extracted from the fit to the 2.76 TeV data. The predicted R_{AA} shows a stronger suppression than the one seen in data. As the authors note in Ref. [42], a K value needed to reproduce the CMS data is about 10% smaller than the one used. This indicates that the medium created at the higher collision energy is closer to the ideal limit, $\hat{q} \simeq 2\epsilon^{3/4}$ [46], where ϵ is the energy density of the QGP. Finally, the V-USPHYDRO+BBMG model [43] couples event-by-event hydrodynamic flow and energy density profiles calculated with V-USPHYDRO [47] to the BBMG jet-energy-loss framework [48]. For the curve shown in Fig. 4, it is assumed that the jet energy loss is proportional to the distance travelled in the medium, that the shear viscosity to entropy density ratio of the medium is 0.05 (less than the Kovtun-Son-Starinets boundary of $1/4\pi$ [49]), and that the freeze-out temperature is 160 MeV. The predicted R_{AA} describes the data well lying on the lower edge of the range covered by the systematic uncertainties of the measurement.

The evolution of central R_{AA} with the collision center-of-mass energy, from the SPS [3, 4] to RHIC [50, 51], and then to the LHC [9–11], is presented in Fig. 5. The data from WA98 and PHENIX are for neutral pions, while the data given by NA49 and STAR are for charged pions and hadrons, respectively. The results from the present analysis are shown by the black dots. The error bars show the statistical uncertainties, while the yellow band surrounding the new $\sqrt{s_{NN}} = 5.02$ TeV CMS points represents the systematic uncertainties, including that of the integrated luminosity (in the previous figures the luminosity uncertainty is shown along with the T_{AA} uncertainty as a separate error box around unity). The T_{AA} uncertainties, which are less than 5%, are not included in the figure. The prediction of the models of Refs. [38–43] at $\sqrt{s_{NN}} = 5.02$ TeV are also shown. The measured nuclear modification factors at all energies show a rising trend at low p_T up to 2 GeV, followed by local minima at RHIC and the LHC at around 7 GeV. At higher p_T , both the RHIC and LHC data show an increase of R_{AA} with increasing p_T .

As the collision energy increases, high p_T charged-particle spectra flatten and extend to larger values. If the average energy loss of a particle at a given p_T is fixed, this flattening would cause R_{AA} to exhibit less suppression. The similar R_{AA} values measured at 2.76 and 5.02 TeV indicate that the effect of flattening spectra could be balanced by a larger average energy loss in the

higher-energy collisions at a fixed p_T [2]. A similar argument could explain the relatively close proximity of the 200 GeV PHENIX and 5.02 TeV CMS measurements for particle $p_T > 10$ GeV, despite the latter having 25 times the collision energy.

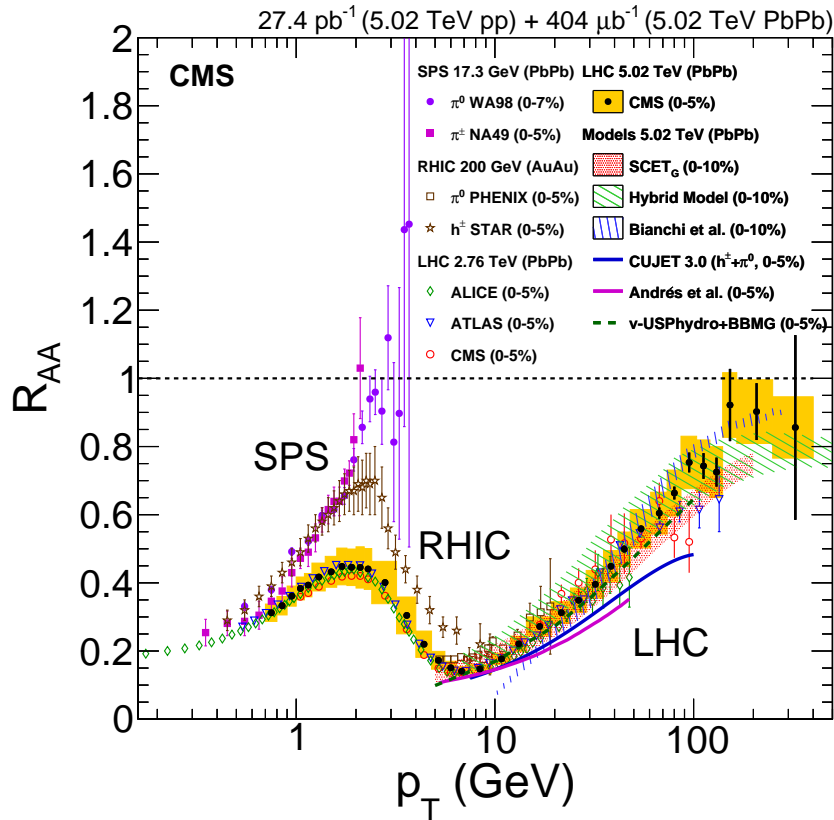


Figure 5: Measurements of the nuclear modification factors in central heavy-ion collisions at four different center-of-mass energies, for neutral pions (SPS, RHIC), charged hadrons (h^\pm) (SPS, RHIC), and charged particles (LHC), from Refs. [3, 4, 9–11, 50–52], compared to predictions of six models for $\sqrt{s_{NN}} = 5.02$ TeV PbPb collisions from Refs. [38–43]. The error bars represent the statistical uncertainties. The yellow band around the 5.02 TeV CMS data points show the systematic uncertainties of this measurement, including that of the integrated luminosity. The T_{AA} uncertainties, of the order of $\pm 5\%$, are not shown. Percentage values in parentheses indicate centrality ranges.

In order to better understand the relationship between the strong suppression seen in R_{AA} and potential cold nuclear matter effects, a previous R_{pA}^* measurement, using 35 nb^{-1} of pPb data at $\sqrt{s_{NN}} = 5.02$ TeV and an interpolated pp reference [13], is recalculated using the pp reference spectrum measured in this paper at $\sqrt{s} = 5.02$ TeV. In order to do this, the corrections for the finite size of the p_T bins applied to the published pPb data are removed, as such a correction is not applied to the pp spectrum measured here. An additional correction for the particle species composition in pPb collisions is calculated and applied in a fashion similar to the measured pp spectrum. The previously published data [13] took this effect into account with a systematic uncertainty, but the correction is applied here in order to benefit from potential cancellations arising from the use of similar analysis procedures on both spectra. The systematic uncertainty due to the particle composition effect was then updated in order to reflect the presence of this additional correction. Figure 6 shows the comparison between the nuclear modification factors in inclusive pPb and PbPb collisions at $\sqrt{s_{NN}} = 5.02$ TeV. At $p_T < 2$ GeV a rising trend is seen in both systems, which in PbPb collisions is followed by a pronounced suppression in the $2 <$

$p_T < 10$ GeV region, and a rising trend from around 10 GeV to the highest p_T . In the pPb system, there is no suppression in the intermediate p_T region, suggesting that in PbPb collisions the suppression is a hot medium effect. Above $p_T > 10$ GeV in the pPb system, a weak momentum dependence is seen leading to a moderate excess above unity at high p_T . This excess is less pronounced than the one seen in R_{pA}^* when using an interpolated pp reference spectrum [13]. At the p_T value of the largest deviation, 65 GeV, R_{pA} is 1.19 ± 0.02 (stat) $^{+0.13}_{-0.11}$ (syst), while R_{pA}^* is 1.41 ± 0.01 (stat) $^{+0.20}_{-0.19}$ (syst). The R_{pA} values above unity in the intermediate p_T region are qualitatively similar to other observed enhancements due to the Cronin effect and radial flow in pA and dA systems [37, 53]. Furthermore, the moderate excess above 10 GeV is suggestive of anti-shadowing effects in the nuclear parton distribution function [34].

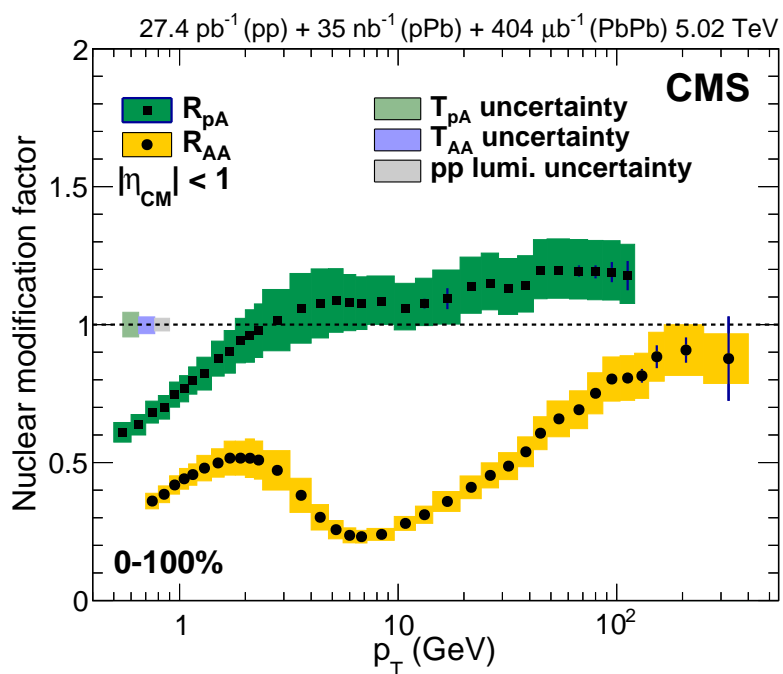


Figure 6: Measurements of the nuclear modification factor for an inclusive centrality class for both PbPb and pPb collisions. The R_{pA} values are formed using the previously published CMS pPb data [13] and the pp reference spectrum described in this paper. Please refer to the main text about the exact procedure followed. The green and yellow boxes show the systematic uncertainties for R_{pA} and R_{AA} , respectively, while the T_{pA} , T_{AA} , and pp luminosity uncertainties are shown as boxes at low p_T around unity.

7 Summary

The transverse momentum spectra of charged particles in pp and PbPb collisions at $\sqrt{s_{NN}} = 5.02$ TeV have been measured in the pseudorapidity window $|\eta| < 1$ in the p_T ranges of 0.5–400 (pp) and 0.7–400 GeV (PbPb). Using these spectra, the nuclear modification factor R_{AA} has been constructed in several bins of collision centrality. In the 0–5% bin, the R_{AA} shows a maximum suppression of a factor of 7–8 around $p_T = 7$ GeV. At higher p_T , it exhibits a rise, reaching a value of $R_{AA} = 0.86 \pm 0.28$ in the p_T bin from 250 to 400 GeV. As collisions become more peripheral, a weakening of both the magnitude and p_T dependence of this suppression is observed. Comparisons of the measured R_{AA} values to the 2.76 TeV results reveal similar p_T dependence and similar suppression. Predictions of the high- p_T R_{AA} coming from the SCET_G,

Hybrid, and v-USPHYDRO+BBMG models are found to approximately reproduce the present data. In central collisions, the CUJET 3.0 model and a model parametrizing the departure of the medium transport coefficient, \hat{q} , from an ideal estimate, both predict R_{AA} suppressions that are slightly larger than seen in data. A model allowing \hat{q} to vary is able to predict the data at high p_T , but expects a larger suppression around 10 GeV. The nuclear modification factor in pPb collisions has been recomputed switching from an interpolation-based reference to the newly measured pp data at $\sqrt{s} = 5.02$ TeV. In the pPb system, in contrast to the PbPb system, no suppression is observed in the 2–10 GeV region. A weak momentum dependence is seen for $p_T > 10$ GeV in the pPb system, leading to a moderate excess above unity at high p_T . The pPb and PbPb nuclear modification factors presented in this paper, covering p_T ranges up to 120 and 400 GeV, respectively, provide stringent constraints on cold and hot nuclear matter effects.

Acknowledgments

We congratulate our colleagues in the CERN accelerator departments for the excellent performance of the LHC and thank the technical and administrative staffs at CERN and at other CMS institutes for their contributions to the success of the CMS effort. In addition, we gratefully acknowledge the computing centers and personnel of the Worldwide LHC Computing Grid for delivering so effectively the computing infrastructure essential to our analyses. Finally, we acknowledge the enduring support for the construction and operation of the LHC and the CMS detector provided by the following funding agencies: BMWFW and FWF (Austria); FNRS and FWO (Belgium); CNPq, CAPES, FAPERJ, and FAPESP (Brazil); MES (Bulgaria); CERN; CAS, MoST, and NSFC (China); COLCIENCIAS (Colombia); MSES and CSF (Croatia); RPF (Cyprus); SENESCYT (Ecuador); MoER, ERC IUT and ERDF (Estonia); Academy of Finland, MEC, and HIP (Finland); CEA and CNRS/IN2P3 (France); BMBF, DFG, and HGF (Germany); GSRT (Greece); OTKA and NIH (Hungary); DAE and DST (India); IPM (Iran); SFI (Ireland); INFN (Italy); MSIP and NRF (Republic of Korea); LAS (Lithuania); MOE and UM (Malaysia); BUAP, CINVESTAV, CONACYT, LNS, SEP, and UASLP-FAI (Mexico); MBIE (New Zealand); PAEC (Pakistan); MSHE and NSC (Poland); FCT (Portugal); JINR (Dubna); MON, RosAtom, RAS and RFBR (Russia); MESTD (Serbia); SEIDI and CPAN (Spain); Swiss Funding Agencies (Switzerland); MST (Taipei); ThEPCenter, IPST, STAR and NSTDA (Thailand); TUBITAK and TAEK (Turkey); NASU and SFFR (Ukraine); STFC (United Kingdom); DOE and NSF (USA).

Individuals have received support from the Marie-Curie programme and the European Research Council and EPLANET (European Union); the Leventis Foundation; the A. P. Sloan Foundation; the Alexander von Humboldt Foundation; the Belgian Federal Science Policy Office; the Fonds pour la Formation à la Recherche dans l’Industrie et dans l’Agriculture (FRIA-Belgium); the Agentschap voor Innovatie door Wetenschap en Technologie (IWT-Belgium); the Ministry of Education, Youth and Sports (MEYS) of the Czech Republic; the Council of Science and Industrial Research, India; the HOMING PLUS programme of the Foundation for Polish Science, cofinanced from European Union, Regional Development Fund, the Mobility Plus programme of the Ministry of Science and Higher Education, the National Science Center (Poland), contracts Harmonia 2014/14/M/ST2/00428, Opus 2013/11/B/ST2/04202, 2014/13/B/ST2/02543 and 2014/15/B/ST2/03998, Sonata-bis 2012/07/E/ST2/01406; the Thalis and Aristeia programmes cofinanced by EU-ESF and the Greek NSRF; the National Priorities Research Program by Qatar National Research Fund; the Programa Clarín-COFUND del Principado de Asturias; the Rachadapisek Sompot Fund for Postdoctoral Fellowship, Chulalongkorn University and the Chulalongkorn Academic into Its 2nd Century Project Advancement Project (Thailand); and the Welch Foundation, contract C-1845.

References

- [1] J. D. Bjorken, "Energy Loss of Energetic Partons in Quark-Gluon Plasma: Possible Extinction of High p_T Jets in Hadron-Hadron Collisions", Technical Report FERMILAB-PUB-82-059-T, 1982.
- [2] D. d'Enterria, "Jet quenching", in *Relativistic Heavy Ion Physics*, R. Stock, ed., volume 23, p. 99. 2010. arXiv:0902.2011. Landolt-Börnstein/SpringerMaterials. doi:10.1007/978-3-642-01539-7_16.
- [3] WA98 Collaboration, "Transverse mass distributions of neutral pions from ^{208}Pb -induced reactions at $158\cdot A$ GeV", *Eur. Phys. J. C* **23** (2002) 225, doi:10.1007/s100520100886, arXiv:nucl-ex/0108006.
- [4] D. d'Enterria, "Indications of suppressed high p_T hadron production in nucleus - nucleus collisions at CERN-SPS", *Phys. Lett. B* **596** (2004) 32, doi:10.1016/j.physletb.2004.06.071, arXiv:nucl-ex/0403055.
- [5] BRAHMS Collaboration, "Quark gluon plasma and color glass condensate at RHIC? The perspective from the BRAHMS experiment", *Nucl. Phys. A* **757** (2005) 1, doi:10.1016/j.nuclphysa.2005.02.130, arXiv:nucl-ex/0410020.
- [6] PHOBOS Collaboration, "The PHOBOS perspective on discoveries at RHIC", *Nucl. Phys. A* **757** (2005) 28, doi:10.1016/j.nuclphysa.2005.03.084, arXiv:nucl-ex/0410022.
- [7] STAR Collaboration, "Experimental and theoretical challenges in the search for the quark gluon plasma: The STAR collaboration's critical assessment of the evidence from RHIC collisions", *Nucl. Phys. A* **757** (2005) 102, doi:10.1016/j.nuclphysa.2005.03.085, arXiv:nucl-ex/0501009.
- [8] PHENIX Collaboration, "Formation of dense partonic matter in relativistic nucleus nucleus collisions at RHIC: Experimental evaluation by the PHENIX collaboration", *Nucl. Phys. A* **757** (2005) 184, doi:10.1016/j.nuclphysa.2005.03.086, arXiv:nucl-ex/0410003.
- [9] ALICE Collaboration, "Centrality dependence of charged particle production at large transverse momentum in Pb–Pb collisions at $\sqrt{s_{\text{NN}}} = 2.76$ TeV", *Phys. Lett. B* **720** (2013) 52, doi:10.1016/j.physletb.2013.01.051, arXiv:1208.2711.
- [10] ATLAS Collaboration, "Measurement of charged-particle spectra in Pb+Pb collisions at $\sqrt{s_{\text{NN}}} = 2.76$ TeV with the ATLAS detector at the LHC", *JHEP* **09** (2015) 050, doi:10.1007/JHEP09(2015)050, arXiv:1504.04337.
- [11] CMS Collaboration, "Study of high- p_T charged particle suppression in PbPb compared to pp collisions at $\sqrt{s_{\text{NN}}} = 2.76$ TeV", *Eur. Phys. J. C* **72** (2012) 1945, doi:10.1140/epjc/s10052-012-1945-x, arXiv:1202.2554.
- [12] M. L. Miller, K. Reygers, S. J. Sanders, and P. Steinberg, "Glauber modeling in high energy nuclear collisions", *Ann. Rev. Nucl. Part. Sci.* **57** (2007) 205, doi:10.1146/annurev.nucl.57.090506.123020, arXiv:nucl-ex/0701025.
- [13] CMS Collaboration, "Nuclear effects on the transverse momentum spectra of charged particles in pPb collisions at $\sqrt{s_{\text{NN}}} = 5.02$ TeV", *Eur. Phys. J. C* **75** (2015) 237, doi:10.1140/epjc/s10052-015-3435-4.

- [14] ATLAS Collaboration, “Transverse momentum, rapidity, and centrality dependence of inclusive charged-particle production in $\sqrt{s_{\text{NN}}} = 5.02 \text{ TeV}$ p+Pb collisions measured by the ATLAS experiment”, (2016). arXiv:1605.06436. Submitted to Phys. Lett. B.
- [15] ALICE Collaboration, “Transverse Momentum Distribution and Nuclear Modification Factor of Charged Particles in p-Pb Collisions at $\sqrt{s_{\text{NN}}} = 5.02 \text{ TeV}$ ”, *Phys. Rev. Lett.* **110** (2013) 082302, doi:10.1103/PhysRevLett.110.082302, arXiv:1210.4520.
- [16] CMS Collaboration, “The CMS experiment at the CERN LHC”, *JINST* **3** (2008) S08004, doi:10.1088/1748-0221/3/08/S08004.
- [17] B. Alver et al., “Importance of correlations and fluctuations on the initial source eccentricity in high-energy nucleus-nucleus collisions”, *Phys. Rev. C* **77** (2008) 014906, doi:10.1103/PhysRevC.77.014906, arXiv:0711.3724.
- [18] CMS Collaboration, “Observation and studies of jet quenching in PbPb collisions at nucleon-nucleon center-of-mass energy = 2.76 TeV”, *Phys. Rev. C* **84** (2011) 024906, doi:10.1103/PhysRevC.84.024906, arXiv:1102.1957.
- [19] Particle Data Group, K. A. Olive et al., “Review of Particle Physics”, *Chin. Phys. C* **38** (2014) 090001, doi:10.1088/1674-1137/38/9/090001.
- [20] H. De Vries, C. W. De Jager, and C. De Vries, “Nuclear charge-density-distribution parameters from elastic electron scattering”, *At. Data Nucl. Data Tables* **36** (1987) 495, doi:10.1016/0092-640X(87)90013-1.
- [21] M. Cacciari, G. P. Salam, and G. Soyez, “The anti- k_t jet clustering algorithm”, *JHEP* **04** (2008) 063, doi:10.1088/1126-6708/2008/04/063, arXiv:0802.1189.
- [22] M. Cacciari, G. P. Salam, and G. Soyez, “FastJet user manual”, *Eur. Phys. J. C* **72** (2012) 1896, doi:10.1140/epjc/s10052-012-1896-2, arXiv:1111.6097.
- [23] O. Kodolova, I. Vardanian, A. Nikitenko, and A. Oulianov, “The performance of the jet identification and reconstruction in heavy ions collisions with CMS detector”, *Eur. Phys. J. C* **50** (2007) 117, doi:10.1140/epjc/s10052-007-0223-9.
- [24] CMS Collaboration, “Description and performance of track and primary-vertex reconstruction with the CMS tracker”, *JINST* **9** (2014) P10009, doi:10.1088/1748-0221/9/10/P10009, arXiv:1405.6569.
- [25] CMS Collaboration, “Commissioning of the Particle-Flow reconstruction in Minimum-Bias and Jet Events from pp Collisions at 7 TeV”, CMS Physics Analysis Summary CMS-PAS-PFT-10-002, 2010.
- [26] T. Sjöstrand, S. Mrenna, and P. Z. Skands, “A brief introduction to PYTHIA 8.1”, *Comput. Phys. Commun.* **178** (2008) 852, doi:10.1016/j.cpc.2008.01.036, arXiv:0710.3820.
- [27] CMS Collaboration, “Event generator tunes obtained from underlying event and multiparton scattering measurements”, *Eur. Phys. J. C* **76** (2016) 155, doi:10.1140/epjc/s10052-016-3988-x, arXiv:1512.00815.
- [28] I. P. Lokhtin and A. M. Snigirev, “A model of jet quenching in ultrarelativistic heavy ion collisions and high- p_T hadron spectra at RHIC”, *Eur. Phys. J. C* **45** (2006) 211, doi:10.1140/epjc/s2005-02426-3, arXiv:hep-ph/0506189.

- [29] CMS Collaboration, “Measurement of transverse momentum relative to dijet systems in PbPb and pp collisions at $\sqrt{s_{\text{NN}}} = 2.76 \text{ TeV}$ ”, *JHEP* **01** (2016) 006, doi:10.1007/JHEP01(2016)006, arXiv:1509.09029.
- [30] K. Werner, F.-M. Liu, and T. Pierog, “Parton ladder splitting and the rapidity dependence of transverse momentum spectra in deuteron-gold collisions at RHIC”, *Phys. Rev. C* **74** (2006) 044902, doi:10.1103/PhysRevC.74.044902, arXiv:hep-ph/0506232.
- [31] T. Pierog et al., “EPOS LHC: Test of collective hadronization with data measured at the CERN Large Hadron Collider”, *Phys. Rev. C* **92** (2015) 034906, doi:10.1103/PhysRevC.92.034906, arXiv:1306.0121.
- [32] ALICE Collaboration, “Multi-strange baryon production at mid-rapidity in Pb-Pb collisions at $\sqrt{s_{\text{NN}}} = 2.76 \text{ TeV}$ ”, *Phys. Lett. B* **728** (2014) 216, doi:10.1016/j.physletb.2013.11.048, arXiv:1307.5543. [Corrigendum: doi:10.1016/j.physletb.2014.05.052.]
- [33] CMS Collaboration, “Measurement of Tracking Efficiency”, CMS Physics Analysis Summary CMS-PAS-TRK-10-002, 2010.
- [34] M. Arneodo, “Nuclear effects in structure functions”, *Phys. Rep.* **240** (1994) 301, doi:10.1016/0370-1573(94)90048-5.
- [35] CMS Collaboration, “Measurement of the elliptic anisotropy of charged particles produced in PbPb collisions at $\sqrt{s_{\text{NN}}} = 2.76 \text{ TeV}$ ”, *Phys. Rev. C* **87** (2013) 014902, doi:10.1103/PhysRevC.87.014902, arXiv:1204.1409.
- [36] J. W. Cronin et al., “Production of hadrons at large transverse momentum at 200, 300, and 400 GeV”, *Phys. Rev. D* **11** (1975) 3105, doi:10.1103/PhysRevD.11.3105.
- [37] PHENIX Collaboration, “Spectra and ratios of identified particles in Au+Au and d+Au collisions at $\sqrt{s_{\text{NN}}} = 200 \text{ GeV}$ ”, *Phys. Rev. C* **88** (2013) 024906, doi:10.1103/PhysRevC.88.024906, arXiv:1304.3410.
- [38] Y.-T. Chien et al., “Jet quenching from QCD evolution”, *Phys. Rev. D* **93** (2016) 074030, doi:10.1103/PhysRevD.93.074030, arXiv:1509.02936.
- [39] J. Casalderrey-Solana et al., “A hybrid strong/weak coupling approach to jet quenching”, *JHEP* **10** (2014) 019, doi:10.1007/JHEP10(2014)019, arXiv:1405.3864. [Erratum: doi:10.1007/JHEP09(2015)175].
- [40] E. Bianchi et al., “The x and Q^2 dependence of \hat{q} , quasi-particles and the JET puzzle”, (2017). arXiv:1702.00481.
- [41] J. Xu, J. Liao, and M. Gyulassy, “Bridging soft-hard transport properties of quark-gluon plasmas with CUJET3.0”, *JHEP* **02** (2016) 169, doi:10.1007/JHEP02(2016)169, arXiv:1508.00552.
- [42] C. Andrés et al., “Energy versus centrality dependence of the jet quenching parameter \hat{q} at RHIC and LHC: a new puzzle?”, *Eur. Phys. J. C* **76** (2016) 475, doi:10.1140/epjc/s10052-016-4320-5, arXiv:1606.04837.
- [43] J. Noronha-Hostler, B. Betz, J. Noronha, and M. Gyulassy, “Event-by-Event Hydrodynamics + Jet Energy Loss: A Solution to the $R_{\text{AA}} \otimes v_2$ Puzzle”, *Phys. Rev. Lett.* **116** (2016) 252301, doi:10.1103/PhysRevLett.116.252301, arXiv:1602.03788.

- [44] J. Casalderrey-Solana et al., “Angular Structure of Jet Quenching Within a Hybrid Strong/Weak Coupling Model”, (2016). arXiv:1609.05842.
- [45] M. Gyulassy, P. Levai, and I. Vitev, “Jet tomography of Au+Au reactions including multigluon fluctuations”, *Phys. Lett. B* **538** (2002) 282,
doi:10.1016/S0370-2693(02)01990-1, arXiv:nucl-th/0112071.
- [46] R. Baier, “Jet quenching”, *Nucl. Phys. A* **715** (2003) 209,
doi:10.1016/S0375-9474(02)01429-X, arXiv:hep-ph/0209038.
- [47] J. Noronha-Hostler et al., “Bulk viscosity effects in event-by-event relativistic hydrodynamics”, *Phys. Rev. C* **88** (2013) 044916,
doi:10.1103/PhysRevC.88.044916, arXiv:1305.1981.
- [48] B. Betz, M. Gyulassy, and G. Torrieri, “Fourier harmonics of high- p_T particles probing the fluctuating intitial condition geometries in heavy-ion collisions”, *Phys. Rev. C* **84** (2011) 024913, doi:10.1103/PhysRevC.84.024913, arXiv:1102.5416.
- [49] P. Kovtun, D. T. Son, and A. O. Starinets, “Holography and hydrodynamics: Diffusion on stretched horizons”, *JHEP* **10** (2003) 064, doi:10.1088/1126-6708/2003/10/064,
arXiv:hep-th/0309213.
- [50] PHENIX Collaboration, “Neutral pion production with respect to centrality and reaction plane in Au+Au collisions at $\sqrt{s_{NN}} = 200$ GeV”, *Phys. Rev. C* **87** (2013) 034911,
doi:10.1103/PhysRevC.87.034911, arXiv:1208.2254.
- [51] STAR Collaboration, “Transverse-Momentum and Collision-Energy Dependence of High p_T Hadron Suppression in Au+Au COLLISions at Ultrarelativistic Energies”, *Phys. Rev. Lett.* **91** (2003) 172302, doi:10.1103/PhysRevLett.91.172302,
arXiv:nucl-ex/0305015.
- [52] NA49 Collaboration, “High transverse momentum hadron spectra at $\sqrt{s_{NN}} = 17.3$ GeV, in Pb+Pb and p+p collisions”, *Phys. Rev. C* **77** (2008) 034906,
doi:10.1103/PhysRevC.77.034906, arXiv:0711.0547.
- [53] CMS Collaboration, “Evidence for Collective Multiparticle Correlations in pPbCollisions”, *Phys. Rev. Lett.* **115** (2015) 012301,
doi:10.1103/PhysRevLett.115.012301, arXiv:1502.05382.

A The CMS Collaboration

Yerevan Physics Institute, Yerevan, Armenia
V. Khachatryan, A.M. Sirunyan, A. Tumasyan

Institut für Hochenergiephysik, Wien, Austria

W. Adam, E. Asilar, T. Bergauer, J. Brandstetter, E. Brondolin, M. Dragicevic, J. Erö, M. Flechl, M. Friedl, R. Frühwirth¹, V.M. Ghete, C. Hartl, N. Hörmann, J. Hrubec, M. Jeitler¹, A. König, I. Krätschmer, D. Liko, T. Matsushita, I. Mikulec, D. Rabady, N. Rad, B. Rahbaran, H. Rohringer, J. Schieck¹, J. Strauss, W. Waltenberger, C.-E. Wulz¹

Institute for Nuclear Problems, Minsk, Belarus
O. Dvornikov, V. Makarenko, V. Zykunov

National Centre for Particle and High Energy Physics, Minsk, Belarus
V. Mossolov, N. Shumeiko, J. Suarez Gonzalez

Universiteit Antwerpen, Antwerpen, Belgium

S. Alderweireldt, E.A. De Wolf, X. Janssen, J. Lauwers, M. Van De Klundert, H. Van Haevermaet, P. Van Mechelen, N. Van Remortel, A. Van Spilbeeck

Vrije Universiteit Brussel, Brussel, Belgium

S. Abu Zeid, F. Blekman, J. D'Hondt, N. Daci, I. De Bruyn, K. Deroover, S. Lowette, S. Moortgat, L. Moreels, A. Olbrechts, Q. Python, S. Tavernier, W. Van Doninck, P. Van Mulders, I. Van Parijs

Université Libre de Bruxelles, Bruxelles, Belgium

H. Brun, B. Clerbaux, G. De Lentdecker, H. Delannoy, G. Fasanella, L. Favart, R. Goldouzian, A. Grebenyuk, G. Karapostoli, T. Lenzi, A. Léonard, J. Luetic, T. Maerschalk, A. Marinov, A. Randle-conde, T. Seva, C. Vander Velde, P. Vanlaer, D. Vannerom, R. Yonamine, F. Zenoni, F. Zhang²

Ghent University, Ghent, Belgium

A. Cimmino, T. Cornelis, D. Dobur, A. Fagot, G. Garcia, M. Gul, I. Khvastunov, D. Poyraz, S. Salva, R. Schöfbeck, M. Tytgat, W. Van Driessche, E. Yazgan, N. Zaganidis

Université Catholique de Louvain, Louvain-la-Neuve, Belgium

H. Bakhshiansohi, C. Beluffi³, O. Bondu, S. Brochet, G. Bruno, A. Caudron, S. De Visscher, C. Delaere, M. Delcourt, B. Francois, A. Giannanco, A. Jafari, P. Jez, M. Komm, G. Krintiras, V. Lemaitre, A. Magitteri, A. Mertens, M. Musich, C. Nuttens, K. Piotrzkowski, L. Quertenmont, M. Selvaggi, M. Vidal Marono, S. Wertz

Université de Mons, Mons, Belgium

N. Belyi

Centro Brasileiro de Pesquisas Físicas, Rio de Janeiro, Brazil

W.L. Aldá Júnior, F.L. Alves, G.A. Alves, L. Brito, C. Hensel, A. Moraes, M.E. Pol, P. Rebello Teles

Universidade do Estado do Rio de Janeiro, Rio de Janeiro, Brazil

E. Belchior Batista Das Chagas, W. Carvalho, J. Chinellato⁴, A. Custódio, E.M. Da Costa, G.G. Da Silveira⁵, D. De Jesus Damiao, C. De Oliveira Martins, S. Fonseca De Souza, L.M. Huertas Guativa, H. Malbouisson, D. Matos Figueiredo, C. Mora Herrera, L. Mundim, H. Nogima, W.L. Prado Da Silva, A. Santoro, A. Sznajder, E.J. Tonelli Manganote⁴, A. Vilela Pereira

Universidade Estadual Paulista ^a, Universidade Federal do ABC ^b, São Paulo, Brazil
 S. Ahuja^a, C.A. Bernardes^b, S. Dogra^a, T.R. Fernandez Perez Tomei^a, E.M. Gregores^b,
 P.G. Mercadante^b, C.S. Moon^a, S.F. Novaes^a, Sandra S. Padula^a, D. Romero Abad^b, J.C. Ruiz
 Vargas

Institute for Nuclear Research and Nuclear Energy, Sofia, Bulgaria

A. Aleksandrov, R. Hadjiiska, P. Iaydjiev, M. Rodozov, S. Stoykova, G. Sultanov, M. Vutova

University of Sofia, Sofia, Bulgaria

A. Dimitrov, I. Glushkov, L. Litov, B. Pavlov, P. Petkov

Beihang University, Beijing, China

W. Fang⁶

Institute of High Energy Physics, Beijing, China

M. Ahmad, J.G. Bian, G.M. Chen, H.S. Chen, M. Chen, Y. Chen⁷, T. Cheng, C.H. Jiang,
 D. Leggat, Z. Liu, F. Romeo, S.M. Shaheen, A. Spiezia, J. Tao, C. Wang, Z. Wang, H. Zhang,
 J. Zhao

State Key Laboratory of Nuclear Physics and Technology, Peking University, Beijing, China

Y. Ban, G. Chen, Q. Li, S. Liu, Y. Mao, S.J. Qian, D. Wang, Z. Xu

Universidad de Los Andes, Bogota, Colombia

C. Avila, A. Cabrera, L.F. Chaparro Sierra, C. Florez, J.P. Gomez, C.F. González Hernández,
 J.D. Ruiz Alvarez, J.C. Sanabria

**University of Split, Faculty of Electrical Engineering, Mechanical Engineering and Naval
 Architecture, Split, Croatia**

N. Godinovic, D. Lelas, I. Puljak, P.M. Ribeiro Cipriano, T. Sculac

University of Split, Faculty of Science, Split, Croatia

Z. Antunovic, M. Kovac

Institute Rudjer Boskovic, Zagreb, Croatia

V. Brigljevic, D. Ferencek, K. Kadija, B. Mesic, S. Micanovic, L. Sudic, T. Susa

University of Cyprus, Nicosia, Cyprus

A. Attikis, G. Mavromanolakis, J. Mousa, C. Nicolaou, F. Ptochos, P.A. Razis, H. Rykaczewski,
 D. Tsiakkouri

Charles University, Prague, Czech Republic

M. Finger⁸, M. Finger Jr.⁸

Universidad San Francisco de Quito, Quito, Ecuador

E. Carrera Jarrin

**Academy of Scientific Research and Technology of the Arab Republic of Egypt, Egyptian
 Network of High Energy Physics, Cairo, Egypt**

A.A. Abdelalim^{9,10}, Y. Mohammed¹¹, E. Salama^{12,13}

National Institute of Chemical Physics and Biophysics, Tallinn, Estonia

M. Kadastik, L. Perrini, M. Raidal, A. Tiko, C. Veelken

Department of Physics, University of Helsinki, Helsinki, Finland

P. Eerola, J. Pekkanen, M. Voutilainen

Helsinki Institute of Physics, Helsinki, Finland

J. Härkönen, T. Järvinen, V. Karimäki, R. Kinnunen, T. Lampén, K. Lassila-Perini, S. Lehti, T. Lindén, P. Luukka, J. Tuominiemi, E. Tuovinen, L. Wendland

Lappeenranta University of Technology, Lappeenranta, Finland

J. Talvitie, T. Tuuva

IRFU, CEA, Université Paris-Saclay, Gif-sur-Yvette, France

M. Besancon, F. Couderc, M. Dejardin, D. Denegri, B. Fabbro, J.L. Faure, C. Favaro, F. Ferri, S. Ganjour, S. Ghosh, A. Givernaud, P. Gras, G. Hamel de Monchenault, P. Jarry, I. Kucher, E. Locci, M. Machet, J. Malcles, J. Rander, A. Rosowsky, M. Titov, A. Zghiche

Laboratoire Leprince-Ringuet, Ecole Polytechnique, IN2P3-CNRS, Palaiseau, France

A. Abdulsalam, I. Antropov, S. Baffioni, F. Beaudette, P. Busson, L. Cadamuro, E. Chapon, C. Charlot, O. Davignon, R. Granier de Cassagnac, M. Jo, S. Lisniak, P. Miné, M. Nguyen, C. Ochando, G. Ortona, P. Paganini, P. Pigard, S. Regnard, R. Salerno, Y. Sirois, T. Strebler, Y. Yilmaz, A. Zabi

Institut Pluridisciplinaire Hubert Curien, Université de Strasbourg, Université de Haute Alsace Mulhouse, CNRS/IN2P3, Strasbourg, France

J.-L. Agram¹⁴, J. Andrea, A. Aubin, D. Bloch, J.-M. Brom, M. Buttignol, E.C. Chabert, N. Chanon, C. Collard, E. Conte¹⁴, X. Coubez, J.-C. Fontaine¹⁴, D. Gelé, U. Goerlach, A.-C. Le Bihan, K. Skovpen, P. Van Hove

Centre de Calcul de l’Institut National de Physique Nucléaire et de Physique des Particules, CNRS/IN2P3, Villeurbanne, France

S. Gadrat

Université de Lyon, Université Claude Bernard Lyon 1, CNRS-IN2P3, Institut de Physique Nucléaire de Lyon, Villeurbanne, France

S. Beauceron, C. Bernet, G. Boudoul, C.A. Carrillo Montoya, R. Chierici, D. Contardo, B. Courbon, P. Depasse, H. El Mamouni, J. Fan, J. Fay, S. Gascon, M. Gouzevitch, G. Grenier, B. Ille, F. Lagarde, I.B. Laktineh, M. Lethuillier, L. Mirabito, A.L. Pequegnot, S. Perries, A. Popov¹⁵, D. Sabes, V. Sordini, M. Vander Donckt, P. Verdier, S. Viret

Georgian Technical University, Tbilisi, Georgia

T. Toriashvili¹⁶

Tbilisi State University, Tbilisi, Georgia

Z. Tsamalaidze⁸

RWTH Aachen University, I. Physikalisches Institut, Aachen, Germany

C. Autermann, S. Beranek, L. Feld, A. Heister, M.K. Kiesel, K. Klein, M. Lipinski, A. Ostapchuk, M. Preuten, F. Raupach, S. Schael, C. Schomakers, J. Schulz, T. Verlage, H. Weber, V. Zhukov¹⁵

RWTH Aachen University, III. Physikalisches Institut A, Aachen, Germany

A. Albert, M. Brodski, E. Dietz-Laursonn, D. Duchardt, M. Endres, M. Erdmann, S. Erdweg, T. Esch, R. Fischer, A. Güth, M. Hamer, T. Hebbeker, C. Heidemann, K. Hoepfner, S. Knutzen, M. Merschmeyer, A. Meyer, P. Millet, S. Mukherjee, M. Olschewski, K. Padeken, T. Pook, M. Radziej, H. Reithler, M. Rieger, F. Scheuch, L. Sonnenschein, D. Teyssier, S. Thüer

RWTH Aachen University, III. Physikalisches Institut B, Aachen, Germany

V. Cherepanov, G. Flügge, B. Kargoll, T. Kress, A. Künsken, J. Lingemann, T. Müller, A. Nehrkorn, A. Nowack, C. Pistone, O. Pooth, A. Stahl¹⁷

Deutsches Elektronen-Synchrotron, Hamburg, Germany

M. Aldaya Martin, T. Arndt, C. Asawatangtrakuldee, K. Beernaert, O. Behnke, U. Behrens, A.A. Bin Anuar, K. Borras¹⁸, A. Campbell, P. Connor, C. Contreras-Campana, F. Costanza, C. Diez Pardos, G. Dolinska, G. Eckerlin, D. Eckstein, T. Eichhorn, E. Eren, E. Gallo¹⁹, J. Garay Garcia, A. Geiser, A. Gizzko, J.M. Grados Luyando, P. Gunnellini, A. Harb, J. Hauk, M. Hempel²⁰, H. Jung, A. Kalogeropoulos, O. Karacheban²⁰, M. Kasemann, J. Keaveney, C. Kleinwort, I. Korol, D. Krücker, W. Lange, A. Lelek, J. Leonard, K. Lipka, A. Lobanov, W. Lohmann²⁰, R. Mankel, I.-A. Melzer-Pellmann, A.B. Meyer, G. Mittag, J. Mnich, A. Mussgiller, E. Ntomari, D. Pitzl, R. Placakyte, A. Raspereza, B. Roland, M.Ö. Sahin, P. Saxena, T. Schoerner-Sadenius, C. Seitz, S. Spannagel, N. Stefaniuk, G.P. Van Onsem, R. Walsh, C. Wissing

University of Hamburg, Hamburg, Germany

V. Blobel, M. Centis Vignali, A.R. Draeger, T. Dreyer, E. Garutti, D. Gonzalez, J. Haller, M. Hoffmann, A. Junkes, R. Klanner, R. Kogler, N. Kovalchuk, T. Lapsien, T. Lenz, I. Marchesini, D. Marconi, M. Meyer, M. Niedziela, D. Nowatschin, F. Pantaleo¹⁷, T. Peiffer, A. Perieanu, J. Poehlsen, C. Sander, C. Scharf, P. Schleper, A. Schmidt, S. Schumann, J. Schwandt, H. Stadie, G. Steinbrück, F.M. Stober, M. Stöver, H. Tholen, D. Troendle, E. Usai, L. Vanelderen, A. Vanhoefer, B. Vormwald

Institut für Experimentelle Kernphysik, Karlsruhe, Germany

M. Akbiyik, C. Barth, S. Baur, C. Baus, J. Berger, E. Butz, R. Caspart, T. Chwalek, F. Colombo, W. De Boer, A. Dierlamm, S. Fink, B. Freund, R. Friese, M. Giffels, A. Gilbert, P. Goldenzweig, D. Haitz, F. Hartmann¹⁷, S.M. Heindl, U. Husemann, I. Katkov¹⁵, S. Kudella, H. Mildner, M.U. Mozer, Th. Müller, M. Plagge, G. Quast, K. Rabbertz, S. Röcker, F. Roscher, M. Schröder, I. Shvetsov, G. Sieber, H.J. Simonis, R. Ulrich, S. Wayand, M. Weber, T. Weiler, S. Williamson, C. Wöhrmann, R. Wolf

Institute of Nuclear and Particle Physics (INPP), NCSR Demokritos, Aghia Paraskevi, Greece

G. Anagnostou, G. Daskalakis, T. Geralis, V.A. Giakoumopoulou, A. Kyriakis, D. Loukas, I. Topsis-Giotis

National and Kapodistrian University of Athens, Athens, Greece

S. Kesisoglou, A. Panagiotou, N. Saoulidou, E. Tziaferi

University of Ioánnina, Ioánnina, Greece

I. Evangelou, G. Flouris, C. Foudas, P. Kokkas, N. Loukas, N. Manthos, I. Papadopoulos, E. Paradas

MTA-ELTE Lendület CMS Particle and Nuclear Physics Group, Eötvös Loránd University, Budapest, Hungary

N. Filipovic

Wigner Research Centre for Physics, Budapest, Hungary

G. Bencze, C. Hajdu, D. Horvath²¹, F. Sikler, V. Veszprenyi, G. Vesztregombi²², A.J. Zsigmond

Institute of Nuclear Research ATOMKI, Debrecen, Hungary

N. Beni, S. Czellar, J. Karancsi²³, A. Makovec, J. Molnar, Z. Szillasi

University of Debrecen, Debrecen, Hungary

M. Bartók²², P. Raics, Z.L. Trocsanyi, B. Ujvari

National Institute of Science Education and Research, Bhubaneswar, India

S. Bahinipati, S. Choudhury²⁴, P. Mal, K. Mandal, A. Nayak²⁵, D.K. Sahoo, N. Sahoo, S.K. Swain

Panjab University, Chandigarh, India

S. Bansal, S.B. Beri, V. Bhatnagar, R. Chawla, U. Bhawandeep, A.K. Kalsi, A. Kaur, M. Kaur, R. Kumar, P. Kumari, A. Mehta, M. Mittal, J.B. Singh, G. Walia

University of Delhi, Delhi, India

Ashok Kumar, A. Bhardwaj, B.C. Choudhary, R.B. Garg, S. Keshri, S. Malhotra, M. Naimuddin, N. Nishu, K. Ranjan, R. Sharma, V. Sharma

Saha Institute of Nuclear Physics, Kolkata, India

R. Bhattacharya, S. Bhattacharya, K. Chatterjee, S. Dey, S. Dutt, S. Dutta, S. Ghosh, N. Majumdar, A. Modak, K. Mondal, S. Mukhopadhyay, S. Nandan, A. Purohit, A. Roy, D. Roy, S. Roy Chowdhury, S. Sarkar, M. Sharan, S. Thakur

Indian Institute of Technology Madras, Madras, India

P.K. Behera

Bhabha Atomic Research Centre, Mumbai, India

R. Chudasama, D. Dutta, V. Jha, V. Kumar, A.K. Mohanty¹⁷, P.K. Netrakanti, L.M. Pant, P. Shukla, A. Topkar

Tata Institute of Fundamental Research-A, Mumbai, India

T. Aziz, S. Dugad, G. Kole, B. Mahakud, S. Mitra, G.B. Mohanty, B. Parida, N. Sur, B. Sutar

Tata Institute of Fundamental Research-B, Mumbai, India

S. Banerjee, S. Bhowmik²⁶, R.K. Dewanjee, S. Ganguly, M. Guchait, Sa. Jain, S. Kumar, M. Maity²⁶, G. Majumder, K. Mazumdar, T. Sarkar²⁶, N. Wickramage²⁷

Indian Institute of Science Education and Research (IISER), Pune, India

S. Chauhan, S. Dube, V. Hegde, A. Kapoor, K. Kothekar, S. Pandey, A. Rane, S. Sharma

Institute for Research in Fundamental Sciences (IPM), Tehran, Iran

S. Chenarani²⁸, E. Eskandari Tadavani, S.M. Etesami²⁸, A. Fahim²⁹, M. Khakzad, M. Mohammadi Najafabadi, M. Naseri, S. Paktinat Mehdiabadi³⁰, F. Rezaei Hosseinabadi, B. Safarzadeh³¹, M. Zeinali

University College Dublin, Dublin, Ireland

M. Felcini, M. Grunewald

INFN Sezione di Bari ^a, Università di Bari ^b, Politecnico di Bari ^c, Bari, Italy

M. Abbrescia^{a,b}, C. Calabria^{a,b}, C. Caputo^{a,b}, A. Colaleo^a, D. Creanza^{a,c}, L. Cristella^{a,b}, N. De Filippis^{a,c}, M. De Palma^{a,b}, L. Fiore^a, G. Iaselli^{a,c}, G. Maggi^{a,c}, M. Maggi^a, G. Miniello^{a,b}, S. My^{a,b}, S. Nuzzo^{a,b}, A. Pompili^{a,b}, G. Pugliese^{a,c}, R. Radogna^{a,b}, A. Ranieri^a, G. Selvaggi^{a,b}, A. Sharma^a, L. Silvestris^{a,17}, R. Venditti^{a,b}, P. Verwilligen^a

INFN Sezione di Bologna ^a, Università di Bologna ^b, Bologna, Italy

G. Abbiendi^a, C. Battilana, D. Bonacorsi^{a,b}, S. Braibant-Giacomelli^{a,b}, L. Brigliadori^{a,b}, R. Campanini^{a,b}, P. Capiluppi^{a,b}, A. Castro^{a,b}, F.R. Cavallo^a, S.S. Chhibra^{a,b}, G. Codispoti^{a,b}, M. Cuffiani^{a,b}, G.M. Dallavalle^a, F. Fabbri^a, A. Fanfani^{a,b}, D. Fasanella^{a,b}, P. Giacomelli^a, C. Grandi^a, L. Guiducci^{a,b}, S. Marcellini^a, G. Masetti^a, A. Montanari^a, F.L. Navarria^{a,b}, A. Perrotta^a, A.M. Rossi^{a,b}, T. Rovelli^{a,b}, G.P. Siroli^{a,b}, N. Tosi^{a,b,17}

INFN Sezione di Catania ^a, Università di Catania ^b, Catania, Italy

S. Albergo^{a,b}, S. Costa^{a,b}, A. Di Mattia^a, F. Giordano^{a,b}, R. Potenza^{a,b}, A. Tricomi^{a,b}, C. Tuve^{a,b}

INFN Sezione di Firenze ^a, Università di Firenze ^b, Firenze, Italy

G. Barbagli^a, V. Ciulli^{a,b}, C. Civinini^a, R. D'Alessandro^{a,b}, E. Focardi^{a,b}, P. Lenzi^{a,b}, M. Meschini^a, S. Paoletti^a, G. Sguazzoni^a, L. Viliani^{a,b,17}

INFN Laboratori Nazionali di Frascati, Frascati, Italy

L. Benussi, S. Bianco, F. Fabbri, D. Piccolo, F. Primavera¹⁷

INFN Sezione di Genova ^a, Università di Genova ^b, Genova, Italy

V. Calvelli^{a,b}, F. Ferro^a, M. Lo Vetere^{a,b}, M.R. Monge^{a,b}, E. Robutti^a, S. Tosi^{a,b}

INFN Sezione di Milano-Bicocca ^a, Università di Milano-Bicocca ^b, Milano, Italy

L. Brianza^{a,b,17}, F. Brivio^{a,b}, M.E. Dinardo^{a,b}, S. Fiorendi^{a,b,17}, S. Gennai^a, A. Ghezzi^{a,b}, P. Govoni^{a,b}, M. Malberti^{a,b}, S. Malvezzi^a, R.A. Manzoni^{a,b}, D. Menasce^a, L. Moroni^a, M. Paganoni^{a,b}, D. Pedrini^a, S. Pigazzini^{a,b}, S. Ragazzi^{a,b}, T. Tabarelli de Fatis^{a,b}

INFN Sezione di Napoli ^a, Università di Napoli 'Federico II' ^b, Napoli, Italy, Università della Basilicata ^c, Potenza, Italy, Università G. Marconi ^d, Roma, Italy

S. Buontempo^a, N. Cavallo^{a,c}, G. De Nardo, S. Di Guida^{a,d,17}, M. Esposito^{a,b}, F. Fabozzi^{a,c}, F. Fienga^{a,b}, A.O.M. Iorio^{a,b}, G. Lanza^a, L. Lista^a, S. Meola^{a,d,17}, P. Paolucci^{a,17}, C. Sciacca^{a,b}, F. Thyssen^a

INFN Sezione di Padova ^a, Università di Padova ^b, Padova, Italy, Università di Trento ^c, Trento, Italy

P. Azzi^{a,17}, N. Bacchetta^a, L. Benato^{a,b}, D. Bisello^{a,b}, A. Boletti^{a,b}, R. Carlin^{a,b}, P. Checchia^a, M. Dall'Osso^{a,b}, P. De Castro Manzano^a, T. Dorigo^a, U. Dosselli^a, F. Gasparini^{a,b}, U. Gasparini^{a,b}, A. Gozzelino^a, S. Lacaprara^a, M. Margoni^{a,b}, A.T. Meneguzzo^{a,b}, J. Pazzini^{a,b}, N. Pozzobon^{a,b}, P. Ronchese^{a,b}, F. Simonetto^{a,b}, E. Torassa^a, S. Ventura^a, M. Zanetti, P. Zotto^{a,b}, G. Zumerle^{a,b}

INFN Sezione di Pavia ^a, Università di Pavia ^b, Pavia, Italy

A. Braghieri^a, A. Magnani^{a,b}, P. Montagna^{a,b}, S.P. Ratti^{a,b}, V. Re^a, C. Riccardi^{a,b}, P. Salvini^a, I. Vai^{a,b}, P. Vitulo^{a,b}

INFN Sezione di Perugia ^a, Università di Perugia ^b, Perugia, Italy

L. Alunni Solestizi^{a,b}, G.M. Bilei^a, D. Ciangottini^{a,b}, L. Fanò^{a,b}, P. Lariccia^{a,b}, R. Leonardi^{a,b}, G. Mantovani^{a,b}, M. Menichelli^a, A. Saha^a, A. Santocchia^{a,b}

INFN Sezione di Pisa ^a, Università di Pisa ^b, Scuola Normale Superiore di Pisa ^c, Pisa, Italy

K. Androsov^{a,32}, P. Azzurri^{a,17}, G. Bagliesi^a, J. Bernardini^a, T. Boccali^a, R. Castaldi^a, M.A. Ciocci^{a,32}, R. Dell'Orso^a, S. Donato^{a,c}, G. Fedi, A. Giassi^a, M.T. Grippo^{a,32}, F. Ligabue^{a,c}, T. Lomtadze^a, L. Martini^{a,b}, A. Messineo^{a,b}, F. Palla^a, A. Rizzi^{a,b}, A. Savoy-Navarro^{a,33}, P. Spagnolo^a, R. Tenchini^a, G. Tonelli^{a,b}, A. Venturi^a, P.G. Verdini^a

INFN Sezione di Roma ^a, Università di Roma ^b, Roma, Italy

L. Barone^{a,b}, F. Cavallari^a, M. Cipriani^{a,b}, D. Del Re^{a,b,17}, M. Diemoz^a, S. Gelli^{a,b}, E. Longo^{a,b}, F. Margaroli^{a,b}, B. Marzocchi^{a,b}, P. Meridiani^a, G. Organtini^{a,b}, R. Paramatti^a, F. Preiato^{a,b}, S. Rahatlou^{a,b}, C. Rovelli^a, F. Santanastasio^{a,b}

INFN Sezione di Torino ^a, Università di Torino ^b, Torino, Italy, Università del Piemonte Orientale ^c, Novara, Italy

N. Amapane^{a,b}, R. Arcidiacono^{a,c,17}, S. Argiro^{a,b}, M. Arneodo^{a,c}, N. Bartosik^a, R. Bellan^{a,b}, C. Biino^a, N. Cartiglia^a, F. Cenna^{a,b}, M. Costa^{a,b}, R. Covarelli^{a,b}, A. Degano^{a,b}, N. Demaria^a, L. Finco^{a,b}, B. Kiani^{a,b}, C. Mariotti^a, S. Maselli^a, E. Migliore^{a,b}, V. Monaco^{a,b}, E. Monteil^{a,b}, M. Monteno^a, M.M. Obertino^{a,b}, L. Pacher^{a,b}, N. Pastrone^a, M. Pelliccioni^a, G.L. Pinna

Angioni^{a,b}, F. Ravera^{a,b}, A. Romero^{a,b}, M. Ruspa^{a,c}, R. Sacchi^{a,b}, K. Shchelina^{a,b}, V. Sola^a, A. Solano^{a,b}, A. Staiano^a, P. Traczyk^{a,b}

INFN Sezione di Trieste ^a, Università di Trieste ^b, Trieste, Italy

S. Belforte^a, M. Casarsa^a, F. Cossutti^a, G. Della Ricca^{a,b}, A. Zanetti^a

Kyungpook National University, Daegu, Korea

D.H. Kim, G.N. Kim, M.S. Kim, S. Lee, S.W. Lee, Y.D. Oh, S. Sekmen, D.C. Son, Y.C. Yang

Chonbuk National University, Jeonju, Korea

A. Lee

Chonnam National University, Institute for Universe and Elementary Particles, Kwangju, Korea

H. Kim

Hanyang University, Seoul, Korea

J.A. Brochero Cifuentes, T.J. Kim

Korea University, Seoul, Korea

S. Cho, S. Choi, Y. Go, D. Gyun, S. Ha, B. Hong, Y. Jo, Y. Kim, B. Lee, K. Lee, K.S. Lee, S. Lee, J. Lim, S.K. Park, Y. Roh

Seoul National University, Seoul, Korea

J. Almond, J. Kim, H. Lee, S.B. Oh, B.C. Radburn-Smith, S.h. Seo, U.K. Yang, H.D. Yoo, G.B. Yu

University of Seoul, Seoul, Korea

M. Choi, H. Kim, J.H. Kim, J.S.H. Lee, I.C. Park, G. Ryu, M.S. Ryu

Sungkyunkwan University, Suwon, Korea

Y. Choi, J. Goh, C. Hwang, J. Lee, I. Yu

Vilnius University, Vilnius, Lithuania

V. Dudenas, A. Juodagalvis, J. Vaitkus

National Centre for Particle Physics, Universiti Malaya, Kuala Lumpur, Malaysia

I. Ahmed, Z.A. Ibrahim, J.R. Komaragiri, M.A.B. Md Ali³⁴, F. Mohamad Idris³⁵, W.A.T. Wan Abdullah, M.N. Yusli, Z. Zolkapli

Centro de Investigacion y de Estudios Avanzados del IPN, Mexico City, Mexico

H. Castilla-Valdez, E. De La Cruz-Burelo, I. Heredia-De La Cruz³⁶, A. Hernandez-Almada, R. Lopez-Fernandez, R. Magaña Villalba, J. Mejia Guisao, A. Sanchez-Hernandez

Universidad Iberoamericana, Mexico City, Mexico

S. Carrillo Moreno, C. Oropeza Barrera, F. Vazquez Valencia

Benemerita Universidad Autonoma de Puebla, Puebla, Mexico

S. Carpintero, I. Pedraza, H.A. Salazar Ibarguen, C. Uribe Estrada

Universidad Autónoma de San Luis Potosí, San Luis Potosí, Mexico

A. Morelos Pineda

University of Auckland, Auckland, New Zealand

D. Kofcheck

University of Canterbury, Christchurch, New Zealand

P.H. Butler

National Centre for Physics, Quaid-I-Azam University, Islamabad, Pakistan

A. Ahmad, M. Ahmad, Q. Hassan, H.R. Hoorani, W.A. Khan, A. Saddique, M.A. Shah, M. Shoaib, M. Waqas

National Centre for Nuclear Research, Swierk, Poland

H. Bialkowska, M. Bluj, B. Boimska, T. Frueboes, M. Górski, M. Kazana, K. Nawrocki, K. Romanowska-Rybinska, M. Szleper, P. Zalewski

Institute of Experimental Physics, Faculty of Physics, University of Warsaw, Warsaw, Poland

K. Bunkowski, A. Byszuk³⁷, K. Doroba, A. Kalinowski, M. Konecki, J. Krolikowski, M. Misiura, M. Olszewski, M. Walczak

Laboratório de Instrumentação e Física Experimental de Partículas, Lisboa, Portugal

P. Bargassa, C. Beirão Da Cruz E Silva, B. Calpas, A. Di Francesco, P. Faccioli, P.G. Ferreira Parracho, M. Gallinaro, J. Hollar, N. Leonardo, L. Lloret Iglesias, M.V. Nemallapudi, J. Rodrigues Antunes, J. Seixas, O. Toldaiev, D. Vadruccio, J. Varela, P. Vischia

Joint Institute for Nuclear Research, Dubna, Russia

S. Afanasiev, P. Bunin, M. Gavrilenco, I. Golutvin, I. Gorbunov, A. Kamenev, V. Karjavin, A. Lanev, A. Malakhov, V. Matveev^{38,39}, V. Palichik, V. Perelygin, S. Shmatov, S. Shulha, N. Skatchkov, V. Smirnov, N. Voytishin, A. Zarubin

Petersburg Nuclear Physics Institute, Gatchina (St. Petersburg), Russia

L. Chtchipounov, V. Golovtsov, Y. Ivanov, V. Kim⁴⁰, E. Kuznetsova⁴¹, V. Murzin, V. Oreshkin, V. Sulimov, A. Vorobyev

Institute for Nuclear Research, Moscow, Russia

Yu. Andreev, A. Dermenev, S. Gninenko, N. Golubev, A. Karneyeu, M. Kirsanov, N. Krasnikov, A. Pashenkov, D. Tlisov, A. Toropin

Institute for Theoretical and Experimental Physics, Moscow, Russia

V. Epshteyn, V. Gavrilov, N. Lychkovskaya, V. Popov, I. Pozdnyakov, G. Safronov, A. Spiridonov, M. Toms, E. Vlasov, A. Zhokin

Moscow Institute of Physics and Technology

A. Bylinkin³⁹

National Research Nuclear University 'Moscow Engineering Physics Institute' (MEPhI), Moscow, Russia

R. Chistov⁴², O. Markin, S. Polikarpov

P.N. Lebedev Physical Institute, Moscow, Russia

V. Andreev, M. Azarkin³⁹, I. Dremin³⁹, M. Kirakosyan, A. Leonidov³⁹, A. Terkulov

Skobeltsyn Institute of Nuclear Physics, Lomonosov Moscow State University, Moscow, Russia

A. Baskakov, A. Belyaev, E. Boos, A. Ershov, A. Gribushin, A. Kaminskiy⁴³, O. Kodolova, V. Korotkikh, I. Loktin, I. Miagkov, S. Obraztsov, S. Petrushanko, V. Savrin, A. Snigirev, I. Vardanyan

Novosibirsk State University (NSU), Novosibirsk, Russia

V. Blinov⁴⁴, Y. Skovpen⁴⁴, D. Shtol⁴⁴

State Research Center of Russian Federation, Institute for High Energy Physics, Protvino, Russia

I. Azhgirey, I. Bayshev, S. Bitioukov, D. Elumakhov, V. Kachanov, A. Kalinin, D. Konstantinov, V. Krychkine, V. Petrov, R. Ryutin, A. Sobol, S. Troshin, N. Tyurin, A. Uzunian, A. Volkov

University of Belgrade, Faculty of Physics and Vinca Institute of Nuclear Sciences, Belgrade, Serbia

P. Adzic⁴⁵, P. Cirkovic, D. Devetak, M. Dordevic, J. Milosevic, V. Rekovic

Centro de Investigaciones Energéticas Medioambientales y Tecnológicas (CIEMAT), Madrid, Spain

J. Alcaraz Maestre, M. Barrio Luna, E. Calvo, M. Cerrada, M. Chamizo Llatas, N. Colino, B. De La Cruz, A. Delgado Peris, A. Escalante Del Valle, C. Fernandez Bedoya, J.P. Fernández Ramos, J. Flix, M.C. Fouz, P. Garcia-Abia, O. Gonzalez Lopez, S. Goy Lopez, J.M. Hernandez, M.I. Josa, E. Navarro De Martino, A. Pérez-Calero Yzquierdo, J. Puerta Pelayo, A. Quintario Olmeda, I. Redondo, L. Romero, M.S. Soares

Universidad Autónoma de Madrid, Madrid, Spain

J.F. de Trocóniz, M. Missiroli, D. Moran

Universidad de Oviedo, Oviedo, Spain

J. Cuevas, J. Fernandez Menendez, I. Gonzalez Caballero, J.R. González Fernández, E. Palencia Cortezon, S. Sanchez Cruz, I. Suárez Andrés, J.M. Vizan Garcia

Instituto de Física de Cantabria (IFCA), CSIC-Universidad de Cantabria, Santander, Spain

I.J. Cabrillo, A. Calderon, J.R. Castiñeiras De Saa, E. Curras, M. Fernandez, J. Garcia-Ferrero, G. Gomez, A. Lopez Virto, J. Marco, C. Martinez Rivero, F. Matorras, J. Piedra Gomez, T. Rodrigo, A. Ruiz-Jimeno, L. Scodellaro, N. Trevisani, I. Vila, R. Vilar Cortabitarte

CERN, European Organization for Nuclear Research, Geneva, Switzerland

D. Abbaneo, E. Auffray, G. Auzinger, M. Bachtis, P. Baillon, A.H. Ball, D. Barney, P. Bloch, A. Bocci, A. Bonato, C. Botta, T. Camporesi, R. Castello, M. Cepeda, G. Cerminara, M. D'Alfonso, D. d'Enterria, A. Dabrowski, V. Daponte, A. David, M. De Gruttola, A. De Roeck, E. Di Marco⁴⁶, M. Dobson, B. Dorney, T. du Pree, D. Duggan, M. Dünser, N. Dupont, A. Elliott-Peisert, S. Fartoukh, G. Franzoni, J. Fulcher, W. Funk, D. Gigi, K. Gill, M. Girone, F. Glege, D. Gulhan, S. Gundacker, M. Guthoff, J. Hammer, P. Harris, J. Hegeman, V. Innocente, P. Janot, J. Kieseler, H. Kirschenmann, V. Knünz, A. Kornmayer¹⁷, M.J. Kortelainen, K. Kousouris, M. Krammer¹, C. Lange, P. Lecoq, C. Lourenço, M.T. Lucchini, L. Malgeri, M. Mannelli, A. Martelli, F. Meijers, J.A. Merlin, S. Mersi, E. Meschi, P. Milenovic⁴⁷, F. Moortgat, S. Morovic, M. Mulders, H. Neugebauer, S. Orfanelli, L. Orsini, L. Pape, E. Perez, M. Peruzzi, A. Petrilli, G. Petrucciani, A. Pfeiffer, M. Pierini, A. Racz, T. Reis, G. Rolandi⁴⁸, M. Rovere, M. Ruan, H. Sakulin, J.B. Sauvan, C. Schäfer, C. Schwick, M. Seidel, A. Sharma, P. Silva, P. Sphicas⁴⁹, J. Steggemann, M. Stoye, Y. Takahashi, M. Tosi, D. Treille, A. Triossi, A. Tsirou, V. Veckalns⁵⁰, G.I. Veres²², M. Verweij, N. Wardle, H.K. Wöhri, A. Zagozdzinska³⁷, W.D. Zeuner

Paul Scherrer Institut, Villigen, Switzerland

W. Bertl, K. Deiters, W. Erdmann, R. Horisberger, Q. Ingram, H.C. Kaestli, D. Kotlinski, U. Langenegger, T. Rohe

Institute for Particle Physics, ETH Zurich, Zurich, Switzerland

F. Bachmair, L. Bäni, L. Bianchini, B. Casal, G. Dissertori, M. Dittmar, M. Donegà, C. Grab, C. Heidegger, D. Hits, J. Hoss, G. Kasieczka, P. Lecomte[†], W. Lustermann, B. Mangano, M. Marionneau, P. Martinez Ruiz del Arbol, M. Masciovecchio, M.T. Meinhard, D. Meister,

F. Micheli, P. Musella, F. Nessi-Tedaldi, F. Pandolfi, J. Pata, F. Pauss, G. Perrin, L. Perrozzi, M. Quitnat, M. Rossini, M. Schönenberger, A. Starodumov⁵¹, V.R. Tavolaro, K. Theofilatos, R. Wallny

Universität Zürich, Zurich, Switzerland

T.K. Aarrestad, C. Amsler⁵², L. Caminada, M.F. Canelli, A. De Cosa, C. Galloni, A. Hinzmann, T. Hreus, B. Kilminster, J. Ngadiuba, D. Pinna, G. Rauco, P. Robmann, D. Salerno, Y. Yang, A. Zucchetta

National Central University, Chung-Li, Taiwan

V. Candelise, T.H. Doan, Sh. Jain, R. Khurana, M. Konyushikhin, C.M. Kuo, W. Lin, Y.J. Lu, A. Pozdnyakov, S.S. Yu

National Taiwan University (NTU), Taipei, Taiwan

Arun Kumar, P. Chang, Y.H. Chang, Y.W. Chang, Y. Chao, K.F. Chen, P.H. Chen, C. Dietz, F. Fiori, W.-S. Hou, Y. Hsiung, Y.F. Liu, R.-S. Lu, M. Miñano Moya, E. Paganis, A. Psallidas, J.f. Tsai, Y.M. Tzeng

Chulalongkorn University, Faculty of Science, Department of Physics, Bangkok, Thailand

B. Asavapibhop, G. Singh, N. Srimanobhas, N. Suwonjandee

Cukurova University, Adana, Turkey

A. Adiguzel, S. Cerci⁵³, S. Damarseckin, Z.S. Demiroglu, C. Dozen, I. Dumanoglu, S. Girgis, G. Gokbulut, Y. Guler, I. Hos⁵⁴, E.E. Kangal⁵⁵, O. Kara, U. Kiminsu, M. Oglakci, G. Onengut⁵⁶, K. Ozdemir⁵⁷, D. Sunar Cerci⁵³, B. Tali⁵³, H. Topakli⁵⁸, S. Turkcapar, I.S. Zorbakir, C. Zorbilmez

Middle East Technical University, Physics Department, Ankara, Turkey

B. Bilin, S. Bilmis, B. Isildak⁵⁹, G. Karapinar⁶⁰, M. Yalvac, M. Zeyrek

Bogazici University, Istanbul, Turkey

E. Gülmез, M. Kaya⁶¹, O. Kaya⁶², E.A. Yetkin⁶³, T. Yetkin⁶⁴

Istanbul Technical University, Istanbul, Turkey

A. Cakir, K. Cankocak, S. Sen⁶⁵

Institute for Scintillation Materials of National Academy of Science of Ukraine, Kharkov, Ukraine

B. Grynyov

National Scientific Center, Kharkov Institute of Physics and Technology, Kharkov, Ukraine

L. Levchuk, P. Sorokin

University of Bristol, Bristol, United Kingdom

R. Aggleton, F. Ball, L. Beck, J.J. Brooke, D. Burns, E. Clement, D. Cussans, H. Flacher, J. Goldstein, M. Grimes, G.P. Heath, H.F. Heath, J. Jacob, L. Kreczko, C. Lucas, D.M. Newbold⁶⁶, S. Paramesvaran, A. Poll, T. Sakuma, S. Seif El Nasr-storey, D. Smith, V.J. Smith

Rutherford Appleton Laboratory, Didcot, United Kingdom

A. Belyaev⁶⁷, C. Brew, R.M. Brown, L. Calligaris, D. Cieri, D.J.A. Cockerill, J.A. Coughlan, K. Harder, S. Harper, E. Olaiya, D. Petyt, C.H. Shepherd-Themistocleous, A. Thea, I.R. Tomalin, T. Williams

Imperial College, London, United Kingdom

M. Baber, R. Bainbridge, O. Buchmuller, A. Bundock, D. Burton, S. Casasso, M. Citron, D. Colling, L. Corpe, P. Dauncey, G. Davies, A. De Wit, M. Della Negra, R. Di Maria, P. Dunne, A. Elwood, D. Fulyan, Y. Haddad, G. Hall, G. Iles, T. James, R. Lane, C. Laner, R. Lucas⁶⁶,

L. Lyons, A.-M. Magnan, S. Malik, L. Mastrolorenzo, J. Nash, A. Nikitenko⁵¹, J. Pela, B. Penning, M. Pesaresi, D.M. Raymond, A. Richards, A. Rose, C. Seez, S. Summers, A. Tapper, K. Uchida, M. Vazquez Acosta⁶⁸, T. Virdee¹⁷, J. Wright, S.C. Zenz

Brunel University, Uxbridge, United Kingdom

J.E. Cole, P.R. Hobson, A. Khan, P. Kyberd, D. Leslie, I.D. Reid, P. Symonds, L. Teodorescu, M. Turner

Baylor University, Waco, USA

A. Borzou, K. Call, J. Dittmann, K. Hatakeyama, H. Liu, N. Pastika

The University of Alabama, Tuscaloosa, USA

S.I. Cooper, C. Henderson, P. Rumerio, C. West

Boston University, Boston, USA

D. Arcaro, A. Avetisyan, T. Bose, D. Gastler, D. Rankin, C. Richardson, J. Rohlf, L. Sulak, D. Zou

Brown University, Providence, USA

G. Benelli, E. Berry, D. Cutts, A. Garabedian, J. Hakala, U. Heintz, J.M. Hogan, O. Jesus, K.H.M. Kwok, E. Laird, G. Landsberg, Z. Mao, M. Narain, S. Piperov, S. Sagir, E. Spencer, R. Syarif

University of California, Davis, Davis, USA

R. Breedon, G. Breto, D. Burns, M. Calderon De La Barca Sanchez, S. Chauhan, M. Chertok, J. Conway, R. Conway, P.T. Cox, R. Erbacher, C. Flores, G. Funk, M. Gardner, W. Ko, R. Lander, C. Mclean, M. Mulhearn, D. Pellett, J. Pilot, S. Shalhout, J. Smith, M. Squires, D. Stolp, M. Tripathi

University of California, Los Angeles, USA

C. Bravo, R. Cousins, A. Dasgupta, P. Everaerts, A. Florent, J. Hauser, M. Ignatenko, N. Mccoll, D. Saltzberg, C. Schnaible, E. Takasugi, V. Valuev, M. Weber

University of California, Riverside, Riverside, USA

E. Bouvier, K. Burt, R. Clare, J. Ellison, J.W. Gary, S.M.A. Ghiasi Shirazi, G. Hanson, J. Heilman, P. Jandir, E. Kennedy, F. Lacroix, O.R. Long, M. Olmedo Negrete, M.I. Paneva, A. Shrinivas, W. Si, H. Wei, S. Wimpenny, B. R. Yates

University of California, San Diego, La Jolla, USA

J.G. Branson, G.B. Cerati, S. Cittolin, M. Derdzinski, R. Gerosa, A. Holzner, D. Klein, V. Krutelyov, J. Letts, I. Macneill, D. Olivito, S. Padhi, M. Pieri, M. Sani, V. Sharma, S. Simon, M. Tadel, A. Vartak, S. Wasserbaech⁶⁹, C. Welke, J. Wood, F. Würthwein, A. Yagil, G. Zevi Della Porta

University of California, Santa Barbara - Department of Physics, Santa Barbara, USA

N. Amin, R. Bhandari, J. Bradmiller-Feld, C. Campagnari, A. Dishaw, V. Dutta, M. Franco Sevilla, C. George, F. Golf, L. Gouskos, J. Gran, R. Heller, J. Incandela, S.D. Mullin, A. Ovcharova, H. Qu, J. Richman, D. Stuart, I. Suarez, J. Yoo

California Institute of Technology, Pasadena, USA

D. Anderson, J. Bendavid, A. Bornheim, J. Bunn, Y. Chen, J. Duarte, J.M. Lawhorn, A. Mott, H.B. Newman, C. Pena, M. Spiropulu, J.R. Vlimant, S. Xie, R.Y. Zhu

Carnegie Mellon University, Pittsburgh, USA

M.B. Andrews, T. Ferguson, M. Paulini, J. Russ, M. Sun, H. Vogel, I. Vorobiev, M. Weinberg

University of Colorado Boulder, Boulder, USA

J.P. Cumalat, W.T. Ford, F. Jensen, A. Johnson, M. Krohn, T. Mulholland, K. Stenson, S.R. Wagner

Cornell University, Ithaca, USA

J. Alexander, J. Chaves, J. Chu, S. Dittmer, K. Mcdermott, N. Mirman, G. Nicolas Kaufman, J.R. Patterson, A. Rinkevicius, A. Ryd, L. Skinnari, L. Soffi, S.M. Tan, Z. Tao, J. Thom, J. Tucker, P. Wittich, M. Zientek

Fairfield University, Fairfield, USA

D. Winn

Fermi National Accelerator Laboratory, Batavia, USA

S. Abdullin, M. Albrow, G. Apollinari, A. Apresyan, S. Banerjee, L.A.T. Bauerdick, A. Beretvas, J. Berryhill, P.C. Bhat, G. Bolla, K. Burkett, J.N. Butler, H.W.K. Cheung, F. Chlebana, S. Cihangir[†], M. Cremonesi, V.D. Elvira, I. Fisk, J. Freeman, E. Gottschalk, L. Gray, D. Green, S. Grünendahl, O. Gutsche, D. Hare, R.M. Harris, S. Hasegawa, J. Hirschauer, Z. Hu, B. Jayatilaka, S. Jindariani, M. Johnson, U. Joshi, B. Klima, B. Kreis, S. Lammel, J. Linacre, D. Lincoln, R. Lipton, M. Liu, T. Liu, R. Lopes De Sá, J. Lykken, K. Maeshima, N. Magini, J.M. Marraffino, S. Maruyama, D. Mason, P. McBride, P. Merkel, S. Mrenna, S. Nahn, V. O'Dell, K. Pedro, O. Prokofyev, G. Rakness, L. Ristori, E. Sexton-Kennedy, A. Soha, W.J. Spalding, L. Spiegel, S. Stoynev, J. Strait, N. Strobbe, L. Taylor, S. Tkaczyk, N.V. Tran, L. Uplegger, E.W. Vaandering, C. Vernieri, M. Verzocchi, R. Vidal, M. Wang, H.A. Weber, A. Whitbeck, Y. Wu

University of Florida, Gainesville, USA

D. Acosta, P. Avery, P. Bortignon, D. Bourilkov, A. Brinkerhoff, A. Carnes, M. Carver, D. Curry, S. Das, R.D. Field, I.K. Furic, J. Konigsberg, A. Korytov, J.F. Low, P. Ma, K. Matchev, H. Mei, G. Mitselmakher, D. Rank, L. Shchutska, D. Sperka, L. Thomas, J. Wang, S. Wang, J. Yelton

Florida International University, Miami, USA

S. Linn, P. Markowitz, G. Martinez, J.L. Rodriguez

Florida State University, Tallahassee, USA

A. Ackert, J.R. Adams, T. Adams, A. Askew, S. Bein, B. Diamond, S. Hagopian, V. Hagopian, K.F. Johnson, H. Prosper, A. Santra, R. Yohay

Florida Institute of Technology, Melbourne, USA

M.M. Baarmand, V. Bhopatkar, S. Colafranceschi, M. Hohlmann, D. Noonan, T. Roy, F. Yumiceva

University of Illinois at Chicago (UIC), Chicago, USA

M.R. Adams, L. Apanasevich, D. Berry, R.R. Betts, I. Bucinskaite, R. Cavanaugh, O. Evdokimov, L. Gauthier, C.E. Gerber, D.J. Hofman, K. Jung, P. Kurt, C. O'Brien, I.D. Sandoval Gonzalez, P. Turner, N. Varelas, H. Wang, Z. Wu, M. Zakaria, J. Zhang

The University of Iowa, Iowa City, USA

B. Bilki⁷⁰, W. Clarida, K. Dilisiz, S. Durgut, R.P. Gundrajula, M. Haytmyradov, V. Khristenko, J.-P. Merlo, H. Mermerkaya⁷¹, A. Mestvirishvili, A. Moeller, J. Nachtman, H. Ogul, Y. Onel, F. Ozok⁷², A. Penzo, C. Snyder, E. Tiras, J. Wetzel, K. Yi

Johns Hopkins University, Baltimore, USA

I. Anderson, B. Blumenfeld, A. Cocoros, N. Eminizer, D. Fehling, L. Feng, A.V. Gritsan, P. Maksimovic, C. Martin, M. Osherson, J. Roskes, U. Sarica, M. Swartz, M. Xiao, Y. Xin, C. You

The University of Kansas, Lawrence, USA

A. Al-bataineh, P. Baringer, A. Bean, S. Boren, J. Bowen, C. Bruner, J. Castle, L. Forthomme, R.P. Kenny III, S. Khalil, A. Kropivnitskaya, D. Majumder, W. Mcbrayer, M. Murray, S. Sanders, R. Stringer, J.D. Tapia Takaki, Q. Wang

Kansas State University, Manhattan, USA

A. Ivanov, K. Kaadze, Y. Maravin, A. Mohammadi, L.K. Saini, N. Skhirtladze, S. Toda

Lawrence Livermore National Laboratory, Livermore, USA

F. Rebassoo, D. Wright

University of Maryland, College Park, USA

C. Anelli, A. Baden, O. Baron, A. Belloni, B. Calvert, S.C. Eno, C. Ferraioli, J.A. Gomez, N.J. Hadley, S. Jabeen, R.G. Kellogg, T. Kolberg, J. Kunkle, Y. Lu, A.C. Mignerey, F. Ricci-Tam, Y.H. Shin, A. Skuja, M.B. Tonjes, S.C. Tonwar

Massachusetts Institute of Technology, Cambridge, USA

D. Abercrombie, B. Allen, A. Apyan, V. Azzolini, R. Barbieri, A. Baty, R. Bi, K. Bierwagen, S. Brandt, W. Busza, I.A. Cali, Z. Demiragli, L. Di Matteo, G. Gomez Ceballos, M. Goncharov, D. Hsu, Y. Iiyama, G.M. Innocenti, M. Klute, D. Kovalevskyi, K. Krajczar, Y.S. Lai, Y.-J. Lee, A. Levin, P.D. Luckey, B. Maier, A.C. Marini, C. McGinn, C. Mironov, S. Narayanan, X. Niu, C. Paus, C. Roland, G. Roland, J. Salfeld-Nebgen, G.S.F. Stephans, K. Sumorok, K. Tatar, M. Varma, D. Velicanu, J. Veverka, J. Wang, T.W. Wang, B. Wyslouch, M. Yang, V. Zhukova

University of Minnesota, Minneapolis, USA

A.C. Benvenuti, R.M. Chatterjee, A. Evans, A. Finkel, A. Gude, P. Hansen, S. Kalafut, S.C. Kao, Y. Kubota, Z. Lesko, J. Mans, S. Nourbakhsh, N. Ruckstuhl, R. Rusack, N. Tambe, J. Turkewitz

University of Mississippi, Oxford, USA

J.G. Acosta, S. Oliveros

University of Nebraska-Lincoln, Lincoln, USA

E. Avdeeva, R. Bartek⁷³, K. Bloom, D.R. Claes, A. Dominguez⁷³, C. Fangmeier, R. Gonzalez Suarez, R. Kamalieddin, I. Kravchenko, A. Malta Rodrigues, F. Meier, J. Monroy, J.E. Siado, G.R. Snow, B. Stieger

State University of New York at Buffalo, Buffalo, USA

M. Alyari, J. Dolen, J. George, A. Godshalk, C. Harrington, I. Iashvili, J. Kaisen, A. Kharchilava, A. Kumar, A. Parker, S. Rappoccio, B. Roozbahani

Northeastern University, Boston, USA

G. Alverson, E. Barberis, A. Hortiangtham, A. Massironi, D.M. Morse, D. Nash, T. Orimoto, R. Teixeira De Lima, D. Trocino, R.-J. Wang, D. Wood

Northwestern University, Evanston, USA

S. Bhattacharya, O. Charaf, K.A. Hahn, A. Kubik, A. Kumar, N. Mucia, N. Odell, B. Pollack, M.H. Schmitt, K. Sung, M. Trovato, M. Velasco

University of Notre Dame, Notre Dame, USA

N. Dev, M. Hildreth, K. Hurtado Anampa, C. Jessop, D.J. Karmgard, N. Kellams, K. Lannon, N. Marinelli, F. Meng, C. Mueller, Y. Musienko³⁸, M. Planer, A. Reinsvold, R. Ruchti, G. Smith, S. Taroni, M. Wayne, M. Wolf, A. Woodard

The Ohio State University, Columbus, USA

J. Alimena, L. Antonelli, B. Bylsma, L.S. Durkin, S. Flowers, B. Francis, A. Hart, C. Hill, R. Hughes, W. Ji, B. Liu, W. Luo, D. Puigh, B.L. Winer, H.W. Wulsin

Princeton University, Princeton, USA

S. Cooperstein, O. Driga, P. Elmer, J. Hardenbrook, P. Hebda, D. Lange, J. Luo, D. Marlow, T. Medvedeva, K. Mei, M. Mooney, J. Olsen, C. Palmer, P. Piroué, D. Stickland, A. Svyatkovskiy, C. Tully, A. Zuranski

University of Puerto Rico, Mayaguez, USA

S. Malik

Purdue University, West Lafayette, USA

A. Barker, V.E. Barnes, S. Folgueras, L. Gutay, M.K. Jha, M. Jones, A.W. Jung, A. Khatiwada, D.H. Miller, N. Neumeister, J.F. Schulte, X. Shi, J. Sun, F. Wang, W. Xie

Purdue University Calumet, Hammond, USA

N. Parashar, J. Stupak

Rice University, Houston, USA

A. Adair, B. Akgun, Z. Chen, K.M. Ecklund, F.J.M. Geurts, M. Guilbaud, W. Li, B. Michlin, M. Northup, B.P. Padley, R. Redjimi, J. Roberts, J. Rorie, Z. Tu, J. Zabel

University of Rochester, Rochester, USA

B. Betchart, A. Bodek, P. de Barbaro, R. Demina, Y.t. Duh, T. Ferbel, M. Galanti, A. Garcia-Bellido, J. Han, O. Hindrichs, A. Khukhunaishvili, K.H. Lo, P. Tan, M. Verzetti

Rutgers, The State University of New Jersey, Piscataway, USA

A. Agapitos, J.P. Chou, E. Contreras-Campana, Y. Gershtein, T.A. Gómez Espinosa, E. Halkiadakis, M. Heindl, D. Hidas, E. Hughes, S. Kaplan, R. Kunnnawalkam Elayavalli, S. Kyriacou, A. Lath, K. Nash, H. Saka, S. Salur, S. Schnetzer, D. Sheffield, S. Somalwar, R. Stone, S. Thomas, P. Thomassen, M. Walker

University of Tennessee, Knoxville, USA

A.G. Delannoy, M. Foerster, J. Heideman, G. Riley, K. Rose, S. Spanier, K. Thapa

Texas A&M University, College Station, USA

O. Bouhali⁷⁴, A. Celik, M. Dalchenko, M. De Mattia, A. Delgado, S. Dildick, R. Eusebi, J. Gilmore, T. Huang, E. Juska, T. Kamon⁷⁵, R. Mueller, Y. Pakhotin, R. Patel, A. Perloff, L. Perniè, D. Rathjens, A. Rose, A. Safonov, A. Tatarinov, K.A. Ulmer

Texas Tech University, Lubbock, USA

N. Akchurin, C. Cowden, J. Damgov, F. De Guio, C. Dragoiu, P.R. Dudero, J. Faulkner, E. Gurpinar, S. Kunori, K. Lamichhane, S.W. Lee, T. Libeiro, T. Peltola, S. Undleeb, I. Volobouev, Z. Wang

Vanderbilt University, Nashville, USA

S. Greene, A. Gurrola, R. Janjam, W. Johns, C. Maguire, A. Melo, H. Ni, P. Sheldon, S. Tuo, J. Velkovska, Q. Xu

University of Virginia, Charlottesville, USA

M.W. Arenton, P. Barria, B. Cox, J. Goodell, R. Hirosky, A. Ledovskoy, H. Li, C. Neu, T. Sinthuprasith, X. Sun, Y. Wang, E. Wolfe, F. Xia

Wayne State University, Detroit, USA

C. Clarke, R. Harr, P.E. Karchin, J. Sturdy

University of Wisconsin - Madison, Madison, WI, USA

D.A. Belknap, J. Buchanan, C. Caillol, S. Dasu, L. Dodd, S. Duric, B. Gomber, M. Grothe, M. Herndon, A. Hervé, P. Klabbers, A. Lanaro, A. Levine, K. Long, R. Loveless, I. Ojalvo, T. Perry, G.A. Pierro, G. Polese, T. Ruggles, A. Savin, N. Smith, W.H. Smith, D. Taylor, N. Woods

†: Deceased

- 1: Also at Vienna University of Technology, Vienna, Austria
- 2: Also at State Key Laboratory of Nuclear Physics and Technology, Peking University, Beijing, China
- 3: Also at Institut Pluridisciplinaire Hubert Curien, Université de Strasbourg, Université de Haute Alsace Mulhouse, CNRS/IN2P3, Strasbourg, France
- 4: Also at Universidade Estadual de Campinas, Campinas, Brazil
- 5: Also at Universidade Federal de Pelotas, Pelotas, Brazil
- 6: Also at Université Libre de Bruxelles, Bruxelles, Belgium
- 7: Also at Deutsches Elektronen-Synchrotron, Hamburg, Germany
- 8: Also at Joint Institute for Nuclear Research, Dubna, Russia
- 9: Also at Helwan University, Cairo, Egypt
- 10: Now at Zewail City of Science and Technology, Zewail, Egypt
- 11: Now at Fayoum University, El-Fayoum, Egypt
- 12: Also at British University in Egypt, Cairo, Egypt
- 13: Now at Ain Shams University, Cairo, Egypt
- 14: Also at Université de Haute Alsace, Mulhouse, France
- 15: Also at Skobeltsyn Institute of Nuclear Physics, Lomonosov Moscow State University, Moscow, Russia
- 16: Also at Tbilisi State University, Tbilisi, Georgia
- 17: Also at CERN, European Organization for Nuclear Research, Geneva, Switzerland
- 18: Also at RWTH Aachen University, III. Physikalisches Institut A, Aachen, Germany
- 19: Also at University of Hamburg, Hamburg, Germany
- 20: Also at Brandenburg University of Technology, Cottbus, Germany
- 21: Also at Institute of Nuclear Research ATOMKI, Debrecen, Hungary
- 22: Also at MTA-ELTE Lendület CMS Particle and Nuclear Physics Group, Eötvös Loránd University, Budapest, Hungary
- 23: Also at University of Debrecen, Debrecen, Hungary
- 24: Also at Indian Institute of Science Education and Research, Bhopal, India
- 25: Also at Institute of Physics, Bhubaneswar, India
- 26: Also at University of Visva-Bharati, Santiniketan, India
- 27: Also at University of Ruhuna, Matara, Sri Lanka
- 28: Also at Isfahan University of Technology, Isfahan, Iran
- 29: Also at University of Tehran, Department of Engineering Science, Tehran, Iran
- 30: Also at Yazd University, Yazd, Iran
- 31: Also at Plasma Physics Research Center, Science and Research Branch, Islamic Azad University, Tehran, Iran
- 32: Also at Università degli Studi di Siena, Siena, Italy
- 33: Also at Purdue University, West Lafayette, USA
- 34: Also at International Islamic University of Malaysia, Kuala Lumpur, Malaysia
- 35: Also at Malaysian Nuclear Agency, MOSTI, Kajang, Malaysia
- 36: Also at Consejo Nacional de Ciencia y Tecnología, Mexico city, Mexico
- 37: Also at Warsaw University of Technology, Institute of Electronic Systems, Warsaw, Poland
- 38: Also at Institute for Nuclear Research, Moscow, Russia
- 39: Now at National Research Nuclear University 'Moscow Engineering Physics

- Institute' (MEPhI), Moscow, Russia
40: Also at St. Petersburg State Polytechnical University, St. Petersburg, Russia
41: Also at University of Florida, Gainesville, USA
42: Also at P.N. Lebedev Physical Institute, Moscow, Russia
43: Also at INFN Sezione di Padova; Università di Padova; Università di Trento (Trento), Padova, Italy
44: Also at Budker Institute of Nuclear Physics, Novosibirsk, Russia
45: Also at Faculty of Physics, University of Belgrade, Belgrade, Serbia
46: Also at INFN Sezione di Roma; Università di Roma, Roma, Italy
47: Also at University of Belgrade, Faculty of Physics and Vinca Institute of Nuclear Sciences, Belgrade, Serbia
48: Also at Scuola Normale e Sezione dell'INFN, Pisa, Italy
49: Also at National and Kapodistrian University of Athens, Athens, Greece
50: Also at Riga Technical University, Riga, Latvia
51: Also at Institute for Theoretical and Experimental Physics, Moscow, Russia
52: Also at Albert Einstein Center for Fundamental Physics, Bern, Switzerland
53: Also at Adiyaman University, Adiyaman, Turkey
54: Also at Istanbul Aydin University, Istanbul, Turkey
55: Also at Mersin University, Mersin, Turkey
56: Also at Cag University, Mersin, Turkey
57: Also at Piri Reis University, Istanbul, Turkey
58: Also at Gaziosmanpasa University, Tokat, Turkey
59: Also at Ozyegin University, Istanbul, Turkey
60: Also at Izmir Institute of Technology, Izmir, Turkey
61: Also at Marmara University, Istanbul, Turkey
62: Also at Kafkas University, Kars, Turkey
63: Also at Istanbul Bilgi University, Istanbul, Turkey
64: Also at Yildiz Technical University, Istanbul, Turkey
65: Also at Hacettepe University, Ankara, Turkey
66: Also at Rutherford Appleton Laboratory, Didcot, United Kingdom
67: Also at School of Physics and Astronomy, University of Southampton, Southampton, United Kingdom
68: Also at Instituto de Astrofísica de Canarias, La Laguna, Spain
69: Also at Utah Valley University, Orem, USA
70: Also at Argonne National Laboratory, Argonne, USA
71: Also at Erzincan University, Erzincan, Turkey
72: Also at Mimar Sinan University, Istanbul, Istanbul, Turkey
73: Now at The Catholic University of America, Washington, USA
74: Also at Texas A&M University at Qatar, Doha, Qatar
75: Also at Kyungpook National University, Daegu, Korea